PB83-259986

Studies of Dust Cake Formation and Structure in Fabric Filtration

Textile Research Inst., Princeton, NJ

Prepared for

Industrial Environmental Research Lab.
Research Triangle Park, NC

Aug 83

U.S. Department of Commerce
National Technical Information Service
NTIS

TECHNICAL REPORT DATA
(Please read Instructions on the reverse before completing)

1. REPORT NO.	2.	3. RECIPIENT'S ACCESSION NO.
EPA-600/9-81-023		PB83 259986

4. TITLE AND SUBTITLE	5. REPORT DATE
STUDIES OF DUST CAKE FORMATION AND STRUCTURE IN FABRIC FILTRATION	August 1983
	6. PERFORMING ORGANIZATION CODE

7. AUTHOR(S)	8. PERFORMING ORGANIZATION REPORT NO.
Bernard Miller, George Lamb, Peter Costanza, Dudley A. Saville, and Myoung Joon Oak	

9. PERFORMING ORGANIZATION NAME AND ADDRESS	10. PROGRAM ELEMENT NO.
Textile Research Institute P.O. Box 625 Princeton, NJ 08540	11. CONTRACT/GRANT NO. Grant R804926-3

12. SPONSORING AGENCY NAME AND ADDRESS	13. TYPE OF REPORT AND PERIOD COVERED
Industrial Environmental Research Laboratory Office of Research and Development U.S. Environmental Protection Agency Research Triangle Park, NC 27711	14. SPONSORING AGENCY CODE EPA/600/13

15. SUPPLEMENTARY NOTES

16. ABSTRACT

Measurements with composite fabrics in which the upstream layer had a very low packing density (i.e., low fiber volume fraction) support the hypothesis that pressure drop reduction by means of electrical stimulation is due to preferential formation of the dust cake in the region of low packing density. These results were obtained with a bench-scale apparatus using 10-cm diameter fabric patches. Measurements were also made with a napped felt bag, intended to reproduce on a larger scale the low surface density structure. Results for the bag were in essential agreement with those for the patches.

The interdependence of electrical stimulation of fabric filters and intensity of cleaning by reverse-air flow has been studied. While standard commercial felts and woven glass fabrics show only a moderate response to cleaning vigor, pressure drop across the napped felts exhibits a strong dependence on both applied voltage and reverse-air velocity.

In order to determine whether effects of fiber cross-sectional shape on filtration performance were mainly mechanical or electrostatic in origin, filter felts were made with round or lobed cross-section fibers and were coated with gold. The improvements in performance due to the lobes vanished for the coated samples, and penetration increased in some cases by an order of magnitude. The hypothesis that effects due to fiber geometry have a large electrostic component is thus reinforced. The stability of the dust cake also appears to depend on electrostatic forces.

Theoretical studies of capture on single fibers in an electric field have revealed that axial polarization effects, frequently ignored in similar studies, can overwhelm the effects of the more commonly studied radial polarization.

17. KEY WORDS AND DOCUMENT ANALYSIS

a. DESCRIPTORS	b. IDENTIFIERS/OPEN ENDED TERMS	c. COSATI Field/Group

18. DISTRIBUTION STATEMENT	19. SECURITY CLASS *(This Report)*	21. NO. OF PAGES
		60
	20. SECURITY CLASS *(This page)*	22. PRICE

EPA Form 2220-1 (Rev. 4-77) PREVIOUS EDITION IS OBSOLETE

PB83-259986

United States
Environmental Protection
Agency

Industrial Environmental Research
Laboratory
Research Triangle Park NC 27711

Research & Development

EPA-600/9-81-023

EPA

Studies of Dust Cake Formation and Structure in Fabric Filtration

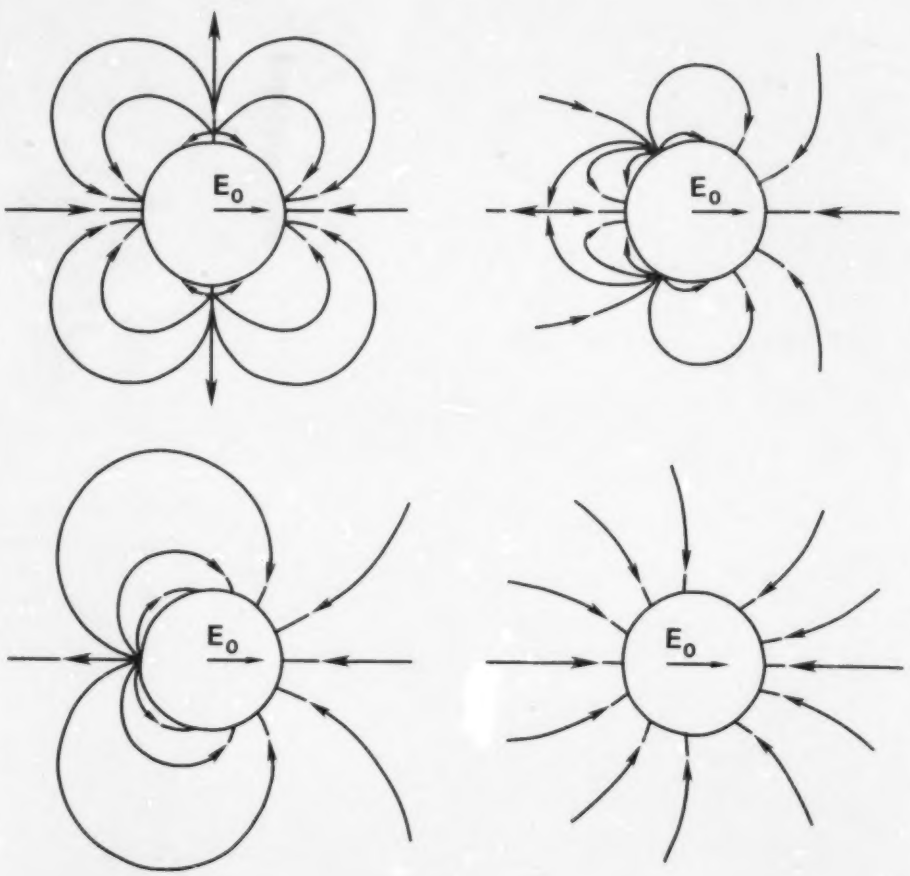

REPRODUCED BY
NATIONAL TECHNICAL
INFORMATION SERVICE
U.S. DEPARTMENT OF COMMERCE
SPRINGFIELD, VA. 22161

EPA-600/9-81-023
August 1983

STUDIES OF DUST CAKE FORMATION AND STRUCTURE IN FABRIC FILTRATION

by

BERNARD MILLER, GEORGE LAMB, PETER COSTANZA, DUDLEY A. SAVILLE, AND MYOUNG JOON OAK

Project Officer

Louis S. Hovis
Utilities and Industrial Processes Division
Industrial Environmental Research Laboratory

**INDUSTRIAL ENVIRONMENTAL RESEARCH LABORATORY
OFFICE OF RESEARCH AND DEVELOPMENT
U.S. ENVIRONMENTAL PROTECTION AGENCY
RESEARCH TRIANGLE PARK, NORTH CAROLINA 27711**

10

DISCLAIMER

This document has been reviewed in accordance with U.S. Environmental Protection Agency policy and approved for publication. Mention of trade names or commercial products does not constitute endorsement or recommendation for use.

FOREWORD

When more and more of our energy and national resources are processed, the impact of pollution on our environment and health requires that more efficient and less costly pollution control methods and devices are developed. EPA's Industrial Environmental Research Laboratory, Research Triangle Park, North Carolina (IERL-RTP), assists in developing improved control methodologies to meet these needs.

This report deals with a laboratory study of a new concept which holds promise for enhanced particulate matter control from coal-fired boilers by fabric filtration. Results of experiments are presented which show that filtration performance can be increased by the imposition of an electric field across the filter cloth in a manner that requires the dust-laden gases to pass through the field. Therein lies the potential for reducing the energy requirements and capital costs for fabric filtration.

Benefits of such research can be realized only when results are applied to commercial units. The authors of this report recommend an immediate study to determine the feasibility of the concept on a larger scale even while recommending the further research that will be necessary to completely define the governing variables.

Frank Princiotta

Frank Princiotta
Director
Industrial Environmental Research Laboratory
Research Triangle Park North Carolina

ABSTRACT

Measurements with composite fabrics in which the upstream layer had a very low packing density (i.e., low fiber volume fraction) support the hypothesis that pressure drop reduction by means of electrical stimulation is due to preferential formation of the dust cake in the region of low packing density. These results were obtained with a bench-scale apparatus using 10-cm diameter fabric patches. Measurements were also made with a napped felt bag, intended to reproduce on a larger scale the low surface density structure. Results for the bag were in essential agreement with those for the patches.

The interdependence of electrical stimulation of fabric filters and intensity of cleaning by reverse-air flow has been studied. While standard commercial felts and woven glass fabrics show only a moderate response to cleaning vigor, pressure drop across napped felts exhibits a strong dependence on both applied voltage and reverse-air velocity.

In order to determine whether effects of fiber cross-sectional shape on filtration performance were mainly mechanical or electrostatic in origin, filter felts were made with round or lobed cross-section fibers and were coated with gold. The improvements in performance due to the lobes vanished for the coated samples, and penetration increased in some cases by an order of magnitude. The hypothesis that effects due to fiber geometry have a large electrostatic component is thus reinforced. The stability of the dust cake also appears to depend on electrostatic forces.

Theoretical studies of capture on single fibers in an electric field have revealed that axial polarization effects, frequently ignored in similar studies, can overwhelm the effects of the more commonly studied radial polarization.

This report was submitted in fulfillment of Grant No. R804926-3 by the Textile Research Institute under the sponsorship of the U.S. Environmental Protection Agency. This report covers the period from December 20, 1978, to December 19, 1979, and work was completed in December 1979.

CONTENTS

Foreword iii
Abstract iv
List of Figures vi
List of Tables viii
Acknowledgements ix

1. Conclusions and Recommendations 1

2. Introduction 2

3. Apparatus 5

4. Effect of Surface Layer Density on Electrical Stimulation 7

5. Electrical Stimulation of a Napped Teflon® Felt Bag 11

6. Effect of Cleaning Intensity on Response to Electrical Stimulation 15

7. Charge Elimination in Lobed-Fiber Filters by Metal Coating 20

8. Calculations of Capture Efficiency of Single Fibers in Electric Fields .. 24
   - Introduction 24
   - Formation of Dendrites 25
   - Collection Efficiency of Single Fibers (Experiments with Uncharged Particles) 30
   - Potential-Induced Charge in a Uniform External Field 35
   - Collection Efficiency for Fibers with Potential-Induced Charges (Uncharged Particles) 37
   - Comparison with Experimental Results 39
   - Collection Efficiency for Fibers with Potential-Induced Charges (Charged Particles) 46

References 49

LIST OF FIGURES

Number		Page
1	Arrangement for holding electrodes against the upstream surface of the patch filter	5
2	Arrangement to provide electrodes in contact with filter bag but not stitched to it	6
3	Dependence of PDR on applied voltage for filters with surface layers of indicated packing density α. Face velocity 3 cm/s.	8
4	Dependence of PDR on applied voltage for filters with surface layers of indicated packing density α. Face velocity 6 cm/s	8
5	Cross section of backing filter used for the composite filters of Figures 3 and 4	9
6	Fiber counts for 0.1-mm intervals down into the cross section in Figure 5	10
7	Pressure drop ratio vs. power needed to obtain it for three combinations of face velocity and surface layer packing density	10
8	Initial and final pressure drops for napped Teflon® bag with and without 4-kV/cm applied field	12
9	Penetration for the bag in Figure 8	12
10	Relationship between ($\Delta P_f - \Delta P_i$) and power dissipated in maintaining the electric field for the napped Teflon® bag of Figures 8 and 9	13
11	Relationship between efficiency and power consumption for the bag in Figures 8–10	14
12	Initial (ΔP_i) and final (ΔP_f) pressure drop for unnapped Teflon® felt at different reverse-air velocities and with different voltages applied between 400-μm diameter wires in contact with the upstream surface	16
13	Like Figure 12, for napped Teflon® felt	16
14	Like Figure 12, for woven glass fabric, J.P. Stevens type 648	17
15	Like Figure 12, for Huyglas® glass felt	17
16	Averages of initial and final pressure drops, ($\Delta P_f - \Delta P_i$)/2, for unnapped and napped Teflon® felts	18
17	Like Figure 16, for type 648 woven glass fabric and Huyglas® glass felt	18
18	Cross-sectional views of three DuPont nylon fibers. Top to bottom: round (AR = 1.0), shallow-lobed trilobal (AR = 1.5), and deep-lobed trilobal (AR = 2.2)	22
19	Penetration of flyash as filtering progresses through fabrics made of the fibers in Figure 18 and through these fabrics after vacuum deposition of gold	23
20	Schematic diagram of apparatus for studying particle capture by a single fiber	24
21	Fiber positions corresponding to Figures 22 and 24	25
22	Dendrite growth on upstream and downstream sides of fiber after filtration for times indicated	26

Number		Page
23	Comparison of measured capture efficiencies (single-fiber experiments) with calculated values	32
24	Particle capture at different locations of fiber tilted 30° from normal position	33
25	Geometry of an off-center fiber between two plate electrodes	35
26	Collection efficiencies for uncharged particles on fibers with potential-induced charges	39
27	Comparison of theory and experiment at d = 0	40
28	Comparison of theory and experiment at d = 0.1 mm	41
29	Comparison of theory and experiment at d = −0.25 mm	42
30	Comparison of theory and experiment at d = −0.8 mm	43
31	Lines of force for uncharged particles near fibers with potential-induced charges at several values of A	45
32	Limiting particle trajectories for charged particles near a fiber with potential-induced charges	47
33	Collection efficiencies for charged particles on fibers with potential-induced charges	48

LIST OF TABLES

Number		Page
1	Comparison of Electrified Teflon® Felt Bags Varying in Surface Density	11
2	Filtration Performance of Gold-Coated Polyester Filter Fabrics after 50 Cycles of Conditioning	20
3	Effects of Lobe Depth and Charge Elimination	23
4	Single-Fiber Capture Efficiency under Different Experimental Conditions	31
5	Comparison of Theoretical and Experimental Collection Efficiencies at Different Distance d from the Centerline	44

ACKNOWLEDGEMENTS

The authors would like to express their appreciation to Dr. James H. Turner for his advice and encouragement throughout the period of this research. They would also like to thank Mr. Harold W. Lambert and Mr. Harry Buvel of Textile Research Institute for their invaluable work on apparatus, Mr. John P. Hession for his assistance with microscopy, and Dr. Harriet G. Heilweil for her help with reports.

SECTION 1
CONCLUSIONS AND RECOMMENDATIONS

This document reports results of studies in electrical stimulation of fabric filtration. The stimulation or enhancement reported was a consequence of the effects of electrostatics on the dust collected and on the collecting fabric. Dust was collected on a filter in the presence of wire electrodes which produced an electric field in the vicinity of the fabric. Various experimental investigations were undertaken, ranging from studies designed to provide an understanding of the basic enhancing mechanism to studies designed to provide a basis for immediate pilot scale development work. The conclusions stated here result from the several kinds of experiments conducted.

As for immediate practical conclusions, experiments showed that the filter fabric construction has a substantial influence on the response of the fabric's performance to electrical stimulation by the electric field. The pressure drop across the filter fabric, considered to be a prime measure of filter performance, is reduced by the presence of a low packing density layer at any given applied external electric field. The pressure drop varies with the packing density of that layer of fabric. To simulate the low packing density layer in a bag filter, experiments were conducted using a needled felt material the upstream surface of which had been napped or brushed vigorously to obtain a "fuzzy" upstream layer. This napped or brushed fabric also proved more sensitive to the intensity of cleaning than smooth fabrics, a characteristic which is in addition to its capacity to lower pressure drop.

Significant conclusions were also inferred from results of experiments the designated objectives of which were to understand the basic mechanism and to explore the range of applicability of electrostatics in enhancement processes. The external field concept was tested on a single fiber, and the relationship between charge and fiber cross-sectional shape was examined. In the latter, application of an electric field caused an increase in particle capture efficiency of a single fiber, but the important implication is that axial polarization plays a greater role in this efficiency increase than does radial polarization. As for fiber shape, the previously recognized improvement in filter performance of fabrics made from fibers of lobed cross-sectional shape is now concluded to be at least partly due to changes on the lobed fabric surface.

Recommendations for further work are a direct consequence of the primary conclusions. As a result of successes in the laboratory, it is recommended that pilot scale testing of electrically stimulated filtration begin immediately using napped or brushed felt bags. Because the bag structure appears to play such an important role, it is recommended that specific fabric development be undertaken. The development would have as a goal a fabric of optimum structure with a low packing density layer on that surface which would ordinarily be positioned upstream in the filtration system. Additional single fiber experiments should be concentrated on determinations of capture efficiencies by single fibers and single fiber arrays under conditions leading to axial fiber polarization.

SECTION 2
INTRODUCTION

This section summarizes the work done during the first two years of a three-year project (Miller *et al.*, 1978 and Miller *et al.*, 1979) and forms the background for the description of the third-year activities which follow. The first two years' work examined (1) how dust deposits in fabric filters and (2) how fiber structure, fabric structure, and externally applied electric fields affect filter performance. Research at Textile Research Institute (TRI) has shown (Miller *et al.*, 1974) that filter performance depends on the geometry of the fibers constituting the filter. Both penetration and pressure drop are reduced when, instead of having the conventional circular shape, the fiber has a lobed cross section, preferably one with three or more lobes. The performance is improved further as the lobes become deeper.

Capture efficiencies of single fibers in uniform electric fields indeed predict that efficiencies of fibers with lobed cross sections should be greater than those of round cross section fibers according to theoretical calculations. Efficiency should increase with number and depth of the lobes, although as the number increases, the increase in efficiency with each additional lobe should decrease rapidly. As the lobe depth increases, efficiency should pass through a maximum when the ratio of the maximum to minimum radial dimension of the cross section is about six. The case in which the number of lobes is two is special. Then, depending on the orientation of the lobes with respect to the direction of gas flow, the efficiency of the lobed fiber could be greater or smaller than that of the round one.

These theoretical results have not been verified by direct experiments with single fibers. However, the similarity between them, as well as results of experiments with felts made of lobed fibers, suggests that the difference in performance due to different fiber cross-sectional shapes may have electrostatic origins. Aerosol particles captured by a filter usually carry charges, so that after a certain amount of initial deposition, particles approaching the filter are captured under the influence of the field due to charges on the previously deposited particles. This hypothesis is difficult to verify quantitatively. The theoretical predictions were derived for clean single fibers, whereas the experiments involve mats of randomly oriented fibers with substantial accumulations of dust. Experimentally, it is found that felt efficiency is higher for trilobal fibers than for round and efficiency increases with lobe depth. But a felt made with bilobal fibers has a lower efficiency than the round-fiber felt. When aerosol particles are discharged, efficiencies of round and trilobal felts become equal. If, on the other hand, extra charges are added to the aerosol, the difference between the efficiencies increases. These facts lend a certain measure of support to the hypothesis that the influence of fiber cross-sectional shape is largely due to electrostatic fields.

The above considerations apply to the influence of fiber shape on efficiency. It is less clear why fiber shape should have an influence on pressure drop, although it seems reasonable to suppose that it is related to cake structure. Photographic approaches to clarify details of this structure have generally been unsuccessful. Direct micrographs of the upstream face of the filter can obviously yield little information about any three dimensional features of the dust deposit. Attempts at making sections through the fabric usually result in disruption of the dust cake either by the cutting action or by the embedding medium. A better approach is to form layered filters whose areal densities add up to that of a filter of interest. After a

certain amount of dust has been deposited in such a layered structure, the layers can be carefully peeled apart and weighed, and the mass of dust deposited in each layer determined. It is assumed that the deposition in a layered structure approximates that in a continuous one. With this method, quantitative data have been obtained about the dependence on various variables of one feature of the dust cake, namely, its mass distribution as a function of distance from the filter surface. It was found that, in a "trilobal" filter, dust is deposited closer to the upstream surface in the first filtration cycle than in a "round" one. Over a number of cycles, this distribution makes for easier removal of the dust by reverse-air flow, so that the amount of dust left embedded in the cloth after cleaning increases more slowly in the trilobal fabric. The experiments were not carried on to the steady state, but it is likely that at that point the round filter would still contain more residual dust and, consequently, exhibit the higher pressure drop that has been observed in comparisons with conditioned trilobal fiber filters.

The principle of obtaining better performance (i.e., lower penetrations and pressure drops) by contriving to make the distribution of dust deposition shift towards the upstream layers was tested in further studies involving filters made of different layers. It was found that when an upstream layer equivalent to 1/6 of the entire filter mass was made of trilobal fibers, while the rest of the filter was made of round fibers, the filter performance was equal to that of a filter made only of trilobal fibers. Similarly, a filter with a 1/6 upstream layer of round fibers and the rest trilobal behaved in the same manner as a round-fiber filter. Thus, the upstream region of a filter apparently dominates behavior. In other measurements, layers of felts made with fine and coarse fibers were combined. When the fine fiber layer was upstream, penetration and pressure drop were both lower than when the filter was reversed, placing the coarse fiber layers upstream. The results obtained over a range of compositions of the layered filters, from all coarse to all fine, showed a good correlation with the mass of dust retained by the filter after cleaning. These results support the view that changes in pressure drop characteristics found with different fiber or fabric structures are related to the dust cake mass and distribution, which in turn are related to the capture efficiency of the fibers. This is especially the case for those fibers in the upstream region of the filter.

Similar considerations are involved in understanding the events by which an external electric field brings about improved filter performance. The Textile Research Institute studied the influence of external electric fields on fabric filtration. The study resulted in development of a technique (referred to as "Electric Stimulation of Fabric Filters" or ESFF) aimed at the improvement of filtration performance at the commercial level. This development has followed empirical lines; the work in this area described in this and previous reports helps to make clear the mechanisms by which the improvements in performance occur. The reason capture efficiency is increased in the presence of an electric field is amply documented. This study has demonstrated that a field perpendicular to both the fiber mat and the flow direction should lead to greater efficiency enhancement (compared with the zero field case) than a field parallel to the flow direction. This is, in fact, the configuration employed in the practical embodiment of the principle being developed at TRI.

The fact that the application of such a field produces a very large decrease in pressure drop seems at first sight another instance of a shift in dust distribution. However, measurements made with layered filters supported this view. In each of these measurements, the upstream layer was fitted with wire electrodes. When the mass distribution of the dust deposits was compared for the cases where 0, 2, 4, and 6 kV were applied between electrodes, it was found that the first layer did collect more dust when the voltages were applied than when none was. However, an important difference between this and the case in which the shift in dust distribution is due to fiber or fabric structure can be illustrated. In the latter case, the differences in pressure drop develop from cycle to cycle as the filters become conditioned, whereas, with an electric field, differences in pressure drop occur in the first cycle. The

explanation based on easier cleaning because of the upstream shift therefore no longer applies. It is in fact replaced by a paradox, since it is hard to see how a concentration of the dust in a narrower region of the fabric can be compatible with lower pressure drop. It would be more reasonable to expect such a concentration to result in reduced cake permeability and increased pressure drop.

The electric fields for these measurements were generated between parallel wire electrodes near the upstream surface of the filter. When a dust cake was formed in the presence of a field, a pattern of stripes was visible. These stripes suggested nonuniform distribution, which could be a possible explanation for the reduced pressure drop, by analogy with the resistance of a number of electric resistors in parallel. This observation was followed by careful experimentation with an apparatus designed to measure the permeability of small areas of dust cake. These experiments showed that the electric field introduced no detectable nonuniformity in the permeability and that the hypothesis must, therefore, be abandoned.

An alternate hypothesis was that the dust distribution, while being shifted in an upstream direction, was also shifted into a region of lower fabric packing density. This would inhibit the formation of a compact dust cake and reduce pressure drop. In other words, by inducing cake formation in a region of the fabric where the packing density is lower, the porosity of the dust cake is increased. This hypothesis is supported by the frequent observation that a fabric having no fuzz on the surface shows no change in pressure drop when an external electric field is applied. Such a filter fabric would typically be one made of untextured continuous filament. In contrast, when the filter fabric has a "nap," the pressure drop responds strongly to an electric field.

SECTION 3
APPARATUS

Two pieces of equipment were used. The first was a "patch" apparatus, in which aerosol was filtered by a small patch of fabric. The filtering area was a circle 10 cm in diameter. The second apparatus was a one-bag baghouse holding a 122-cm long, 11.4-cm diameter bag. In both, pulverized coal flyash was fed continuously into the inlet duct and dispersed by a jet of compressed air. Penetration was determined by sampling outlet aerosol through membrane filters. Pressure was measured with manometers and also continuously recorded.

Both devices simulated baghouse operation by automatically repeating a preset sequence of cleaning and filtering intervals. The baghouse provided for cleaning by pulse-jet only. In the patch apparatus, a choice of reverse-air or pulse-jet cleaning was available. A more detailed description of the equipment was given in a previous report (Miller *et al.*, 1977).

In experiments with electric stimulation, wire electrodes were held against the upstream surface of the fabric. In the patch apparatus the wires were fixed to a round holder pressed against the fabric (Fig. 1). In the baghouse, the electrodes were fabricated into a net-like structure which was laced round the bag and called a corset (Fig. 2).

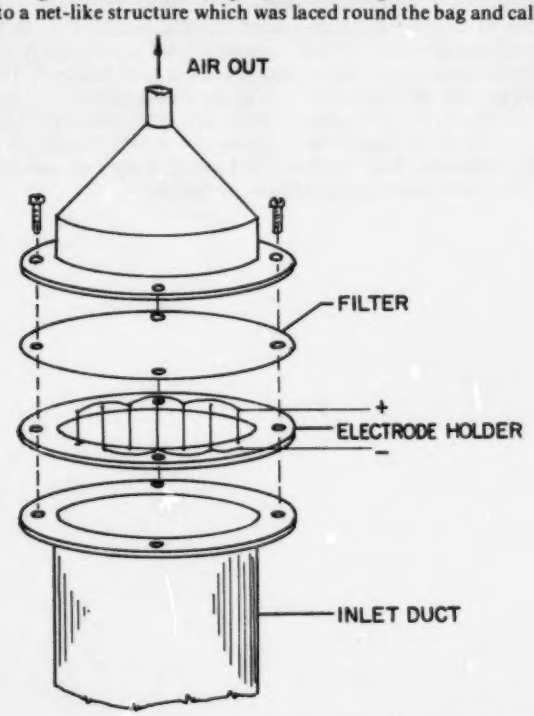

Figure 1. Arrangement for holding electrodes against the upstream surface of the patch filter.

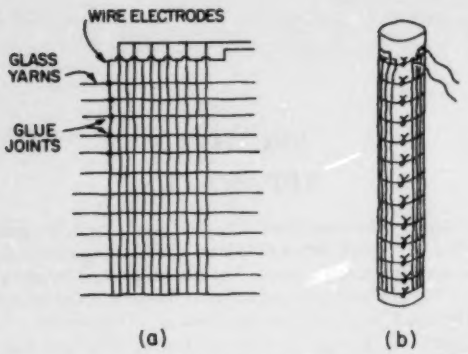

Figure 2. Arrangement to provide electrodes in contact with filter bag but not stitched to it.

a) Formation of assembly. b) Assembly laced on bag.

The apparatus used for measurements of single-fiber efficiencies was designed to deliver a dry aerosol of monodisperse spherical polystyrene particles to the target fiber. A syringe pump fed a dilute suspension of the particles to an atomizer, which was designed to trap all droplets greater than a certain size. In this way, the population of agglomerates in the aerosol could be effectively eliminated by adjusting the concentration of the suspension to a suitably low level. The aerosol was then dried by passing through a tube containing drying agent, and afterward passed either through a neutralizer containing 2 millicurie of Krypton 85 (Thermo-Systems, Inc. Model 3012) or through a corona charger to add charges to the particles. Aerosol concentration was checked by passing a known volume through a membrane filter and weighing the amount collected.

SECTION 4

EFFECT OF SURFACE LAYER DENSITY ON ELECTRICAL STIMULATION

In the preceding report (Miller *et al.*, 1979), the hypothesis was proposed that the lowering of pressure drop due to ESFF depends on the presence of a region having low fiber volume fraction on the upstream surface of the fabric. This was suggested by the observation that needled felts give substantial pressure drop response to ESFF, but cloth woven from continuous filament does not. In another example, a fabric woven so as to have a "rough" and a "smooth" side was found to respond better with the "rough" side upstream. In a third case, glass fabrics gave better response after a nap was raised on the upstream surface. Moreover, photographs (published in the preceding report) showed enhanced collection on the surface layers in the presence of an electric field.

The effect was examined in systematic fashion in the following experiments. Polyester felts were made from card webs bonded with a low softening-point fiber (Vinyon) so as to have different values of packing density α (i.e., volume fraction of fiber). Each of these felts was then combined with a much thicker commercial needled polyester filter fabric to produce a set of layered filters in which the prepared felts were the upstream layer. The procedure could be regarded as a way to vary the surface layer density of the same needled fabric. Each combination was placed in the patch apparatus with the felt surface in contact with 400-μm diameter electrodes fixed to a separate annulus.

After about twenty conditioning cycles, pressure drop characteristics were determined over a range of applied electric fields and at two face velocities. Results for 3 and 6-cm/s face velocity are shown in Figures 3 and 4, respectively. In both cases, there is a strong dependence of the PDR-field curve on the density of the upstream felt layer. It is well at this point to clarify the various terms related to pressure drop used in this report. The difference in pressure between the upstream and downstream sides of a filter is called the pressure drop, sometimes abbreviated as ΔP. Where a filter is run continuously in a sequence of filtering and cleaning steps, the pressure drop during the filtering interval varies between two limits: the initial pressure drop ΔP_i just after the filter has been cleaned and the main flow has resumed, and the final pressure drop ΔP_f at the end of the filtering interval, just before cleaning. $(\Delta P_f - \Delta P_i)$ is called the pressure drop rise. The pressure drop ratio or PDR is the ratio of the rise obtained with an applied field to the rise obtained at zero field.

The points marked with the symbol P are for the backing fabric without a surface felt. These are interesting for two reasons. The overall packing density of the needled fabric was measured and found to be 0.20. However, the fabric behaved in the PDR experiments as if it had a surface layer of smaller density. That this is actually the case is shown by fiber counts made on cross sections of the needled fabric. Figure 5 shows such a cross section and Figure 6 is a plot of fiber counts in 0.1-mm intervals. The surface regions of lower density are seen to be approximately 0.5 mm thick on both sides of the fabric.

It can also be seen that the "P" curve at 6 cm/s corresponds to a higher surface density than at 3 cm/s. This suggests that at the higher face velocity the surface layer of the needled fabric is compressed by the airflow. The objection to this is that the

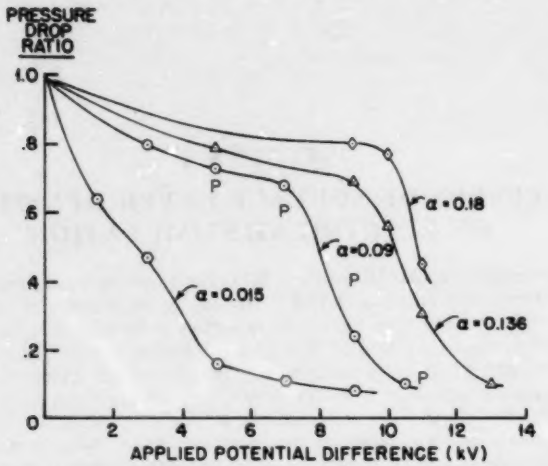

Figure 3. Dependence of PDR on applied volatage for filters with surface layers of indicated packing density α. Points marked "P" are for backing fabric with no added surface layer. Face velocity 3 cm/s.

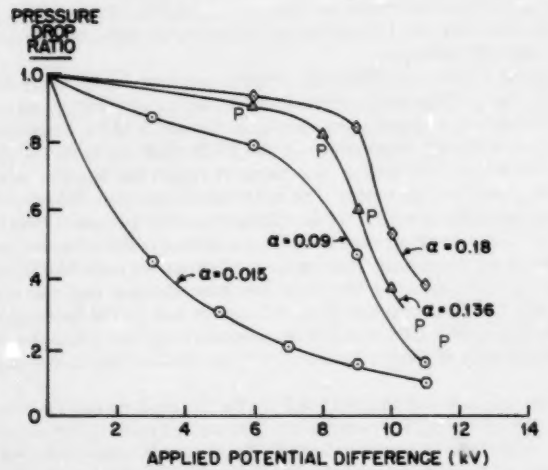

Figure 4. Dependence of PDR on applied voltage for filters with surface layers of indicated packing density α. Points marked "P" are for backing fabric with no added surface layer. Face velocity 6 cm/s.

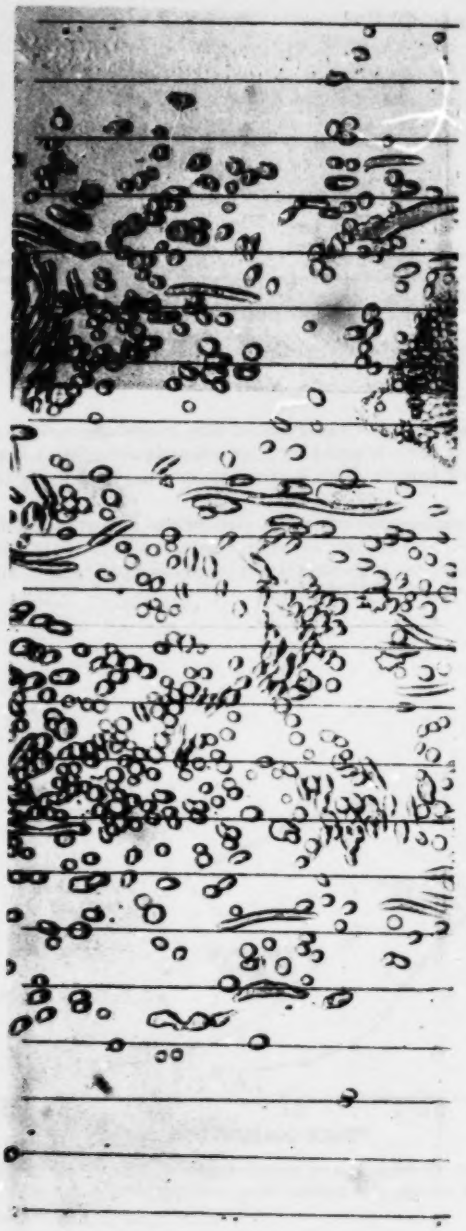

Figure 5. Cross section of backing filter used for the composite filters of Figures 3 and 4.

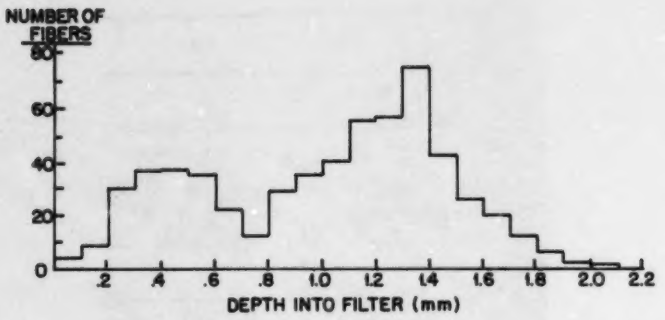

Figure 6. Fiber counts for 0.1-mm intervals down into the cross section in Figure 5.

other surface layers, that is, the prepared felts, should also have been compressed at the higher face velocity. In order for this explanation to hold it is necessary to assume that the needled surface layer is more easily compressed, but this has not been verified.

Power consumption was measured with the two felts of lowest density ($\alpha = 0.015$ and 0.09). These results are plotted in Figure 7, and it is clear that a low-density surface layer may be an important factor in reducing power consumption in ESFF as well as in achieving low PDR values.

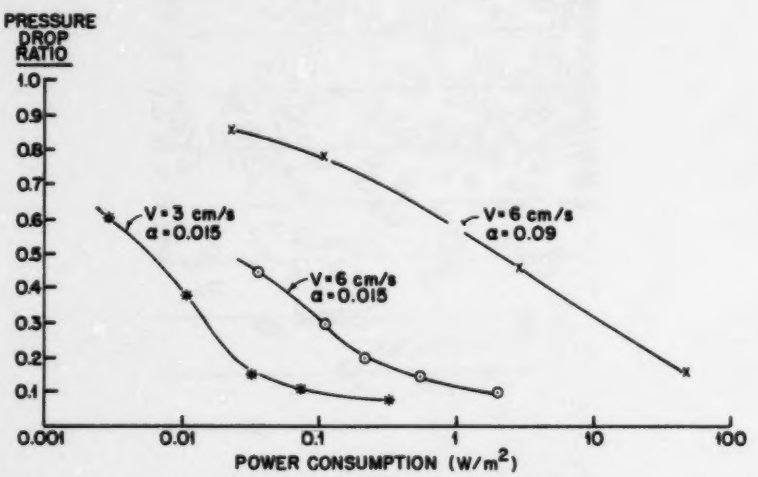

Figure 7. Pressure drop ratio vs. power needed to obtain it for three combinations of face velocity and surface layer packing density.

SECTION 5

ELECTRICAL STIMULATION OF A NAPPED TEFLON® FELT BAG

The next step in these ESFF studies was to verify whether low surface packing density would produce similar improvements in a practical filter bag. Low surface packing density can be obtained by napping or brushing the surface of a felt, and it was decided to use this technique in an initial trial. A standard Teflon® felt (XT-2363, 23 oz/yd^2), prepared by the DuPont Company, was given a low-density surface nap. Such a fabric could then be qualitatively compared to the standard felt. The napped Teflon® felt was then fabricated into a bag and fitted with a 400-μm wire corset with wires 15 mm apart. The experimental conditions were set at values given in Table 1.

Figure 8 shows pressure drops with and without a field up to 400 cycles, and Figure 9 shows the corresponding penetration values for the napped Teflon® bag. (Note that percent penetration is defined as 100 minus percent efficiency, E.) Pressure drops are as low as those obtained in the patch apparatus for low-density surfaces, and electrical power consumption is also of the same order (Table 1). It appears that napping is an effective means of producing a low-density surface to obtain very low pressure drops and electrical power consumptions in the presence of a field.

TABLE 1. COMPARISON OF ELECTRIFIED TEFLON® FELT BAGS VARYING IN SURFACE DENSITY

	Teflon® felt (napped)		Teflon® felt (standard)	
	0 kV	2 kV/cm	0 kV	4.7 kV/cm
ΔP_f (mm H_2O)	21	9	45	15
ΔP_i	7	6	11	8
(ΔP_f - P_i)	14	3	34	7
PDR	-	0.2	-	0.2
Penetration (%)	2.2	0.5 (0.7)*	0.5	0.1
Electrical power required (W/m_2)	-	0.3 (0.1)*	-	0.6

Each bag (0.39 m_2) fitted with corset (400-μm electrodes)

Face velocity: 6 ft/min (3 cm/s)
Inlet conc.: 12.5 g/m^3
Jet pulse pressure: 45 psi (*70 psi)
300 to 400 cycles conditioning
Cycle length: 15 min

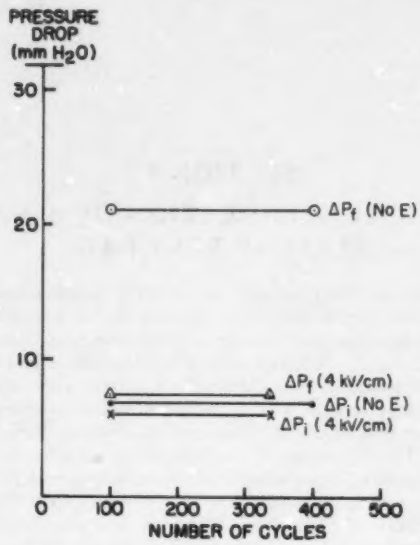

Figure 8. Initial and final pressure drops for napped Teflon® bag with and without 4-kV/cm applied field.

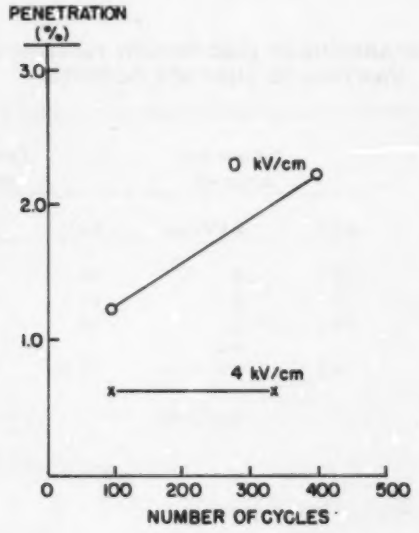

Figure 9. Penetration for the bag in Figure 8.

However, in the absence of a field, the penetration at 400 cycles has increased, presumably because of seepage of increased residual dust; it was not determined whether this increased level of penetration was a steady-state value or was still increasing at the 400th cycle. In addition, this particular napped Teflon® is abnormally higher in penetration without a field than the standard Teflon® bag (see Table 1). It is believed that this is due to excessive vigor in the napping process and should be easily corrected in future trials. Nevertheless, the effects of the nap on other responses to the field are encouraging and justify further study of these fabric structures. Final pressure drop and pressure drop ratio (PDR) are half the values obtained with the standard Teflon® bag. Electrical power can be reduced to half that consumed with the higher density standard felt if the pulse-jet pressure is increased to 70 psi. (The effects of pulse-jet and reverse-air intensity are now being separately studied, and preliminary results are given in another section of this report.)

The variation of performance with field strength was also determined for face velocities ranging from 1.5 cm/s to 6 cm/s. Pressure drop rises ($\Delta P_f - \Delta P_i$) and capture efficiencies are plotted in Figures 10 and 11, respectively, as a function of electrical power consumption due to varying field strength. It can be seen that performance responds immediately at low field strengths and power consumptions for all face velocities. These curves are unlike those for a standard Teflon® bag which required a greater field strength and power consumption to produce such responses. As expected, curves for pressure drop rise are higher and curves for efficiency are lower at higher face velocities, but even at 6 cm/s (12 ft/min) considerable improvements can be obtained at lower power consumption.

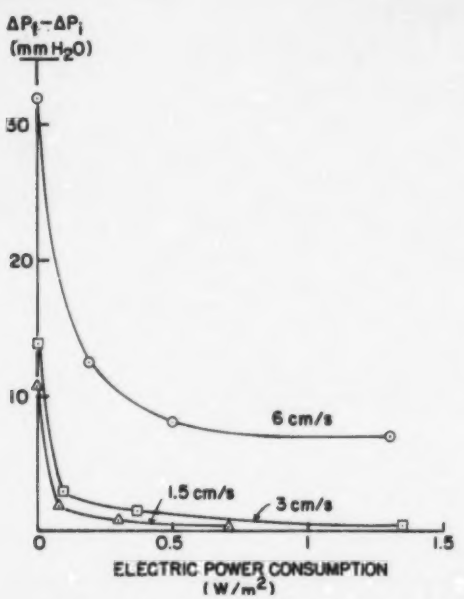

Figure 10. Relationship between ($\Delta P_f - \Delta P_i$) and power dissipated in maintaining the electric field for the napped Teflon® bag in Figures 8 and 9.

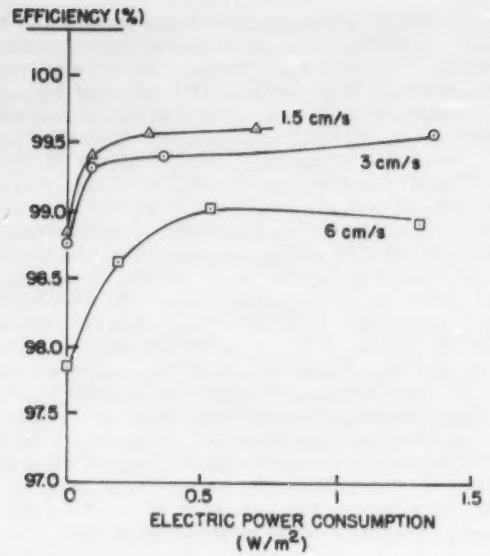

Figure 11. Relationship between efficiency and power consumption for the bag in Figures 8–10.

SECTION 6

EFFECT OF CLEANING INTENSITY ON RESPONSE TO ELECTRICAL STIMULATION

Previously reported studies on ESFF focused on the effects of numerous process variables, such as voltage, face velocity, and length of conditioning. The cleaning step has not been systematically investigated, and in most cases, reverse-air velocity or pulse intensity has been kept constant. Recent evidence has brought to light a possible strong relationship between the effects of ESFF and the degree of cleaning.

In addition, an important question concerning the effectiveness of ESFF in lowering the initial pressure drop must be considered. ESFF-pressure drop relationships have been reported in terms of the pressure drop ratio (PDR), which is the ratio of the pressure drop rise with an applied field to that without an electric field. The value just after cleaning (the initial pressure drop, ΔP_i) was not considered in itself, since its value could be arbitrarily varied and since it was, in any case, only a minor fraction of the maximum ΔP_f. This, however, is not the case in actual operations, where values of ΔP_i may be greater than 50% of ΔP_f values and are subject to slow increases over periods of months and years. In such cases, if ESFF acted only to reduce ($\Delta P_f - \Delta P_i$), the benefits of ESFF would be smaller than might be expected from consideration of PDR values. It was decided, therefore, to initiate determinations of the relationships between cleaning, PDR, and both ΔP_i and ΔP_f, in order to determine their relevance to existing filter fabrics.

The TRI patch apparatus was used for these measurements. A flow meter was introduced into the reverse-air line, and pressure drop performance was measured over a range of applied voltages and reverse-air flows. Fabrics used included a standard Teflon® felt, a Teflon® felt whose surface had been napped, a woven glass fabric of "648" construction from J.P. Stevens & Co. Inc., and a Huyglas® glass fiber felt produced by Huyck Corporation. In these studies the forward face velocity was maintained at 3 cm/s in all cases.

Figure 12 shows the results for the standard Teflon® felt. Reverse-air velocity ranged from about 1.25 to about 2.25 times the forward velocity. Within this range, increasing the reverse velocity reduced both ΔP_i and ΔP_f, and application of the field reduced ΔP_f but not ΔP_i. Figure 13 shows the results for the Teflon® felt with a napped upstream surface, which are in interesting contrast to those in Figure 12. At a reverse-air velocity of 4 cm/s, there is a strong dependence of both ΔP_i and ΔP_f on the applied voltage. In the absence of an applied field, both ΔP_i and ΔP_f rise to rather high values, much higher than those for the standard felt. As the reverse-air velocity is increased, all pressure drops fall rather quickly to values lower than those for the standard felt. With a 6-kV/cm applied field, the pressure drop becomes almost independent of the reverse-air velocity and remains at an exceptionally low value.

Results obtained with the woven glass fabric are shown in Figure 14. With this material, there was a sharp decrease in pressure drop with increased reverse-air velocity, and some sensitivity of ΔP_f to applied voltage was apparent. Figure 15 shows the results for the Huyglas® fabric. The response to applied field with this material was comparable to that of the standard Teflon® felt.

Figures 16 and 17 show the same data as in Figures 12–15 condensed by being plotted as average ΔP values, i.e., each point in Figures 16 and 17 is the average of the corresponding ΔP_i and ΔP_f values shown in the previous figures. These values are

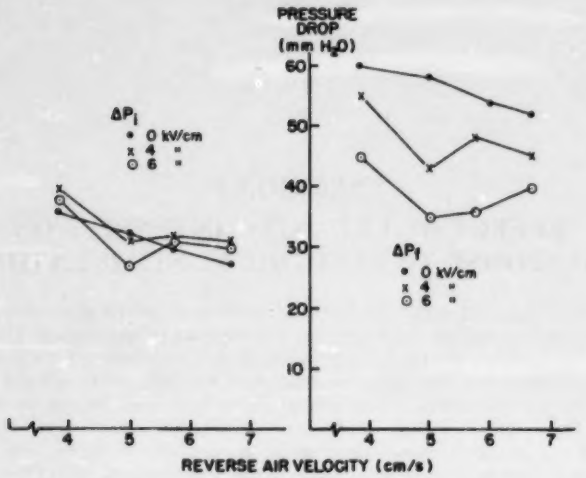

Figure 12. Initial (ΔP_i) and final (ΔP_f) pressure drop for unnapped Teflon® felt at different reverse-air velocities and with different voltages applied between 400-μm diameter wires in contact with the upstream surface.

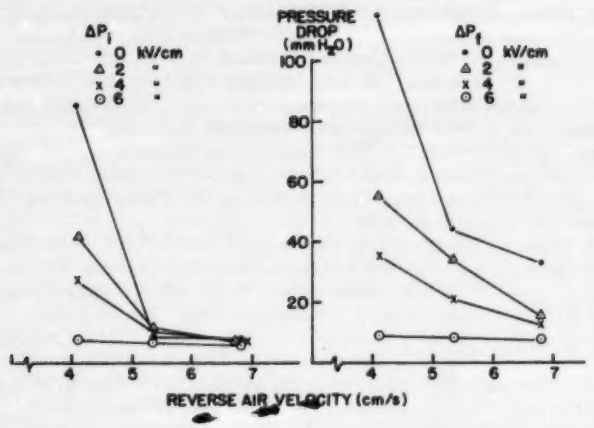

Figure 13. Like Figure 12, for napped Teflon® felt.

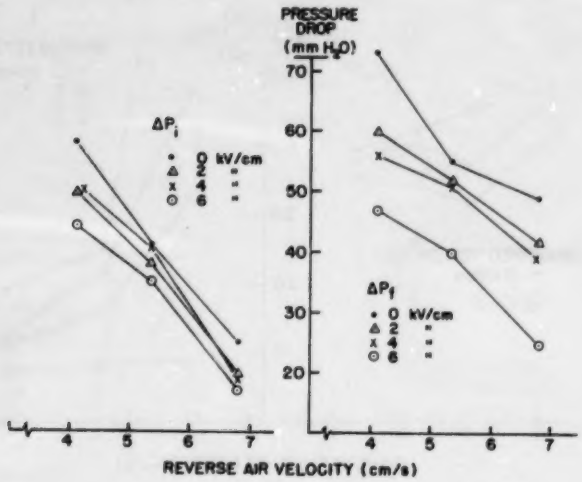

Figure 14. Like Figure 12, for woven glass fabric, J. P. Stevens type 648.

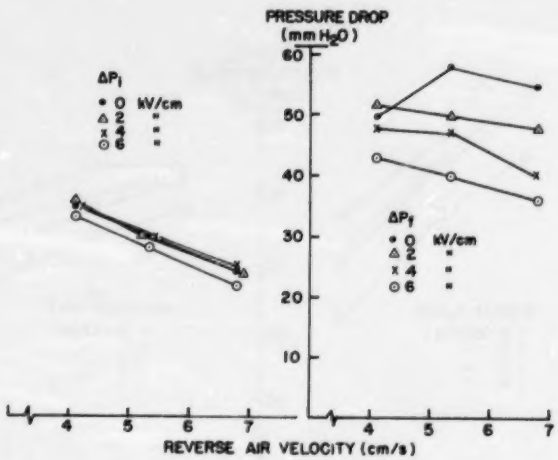

Figure 15. Like Figure 12, for Huyglas® glass felt.

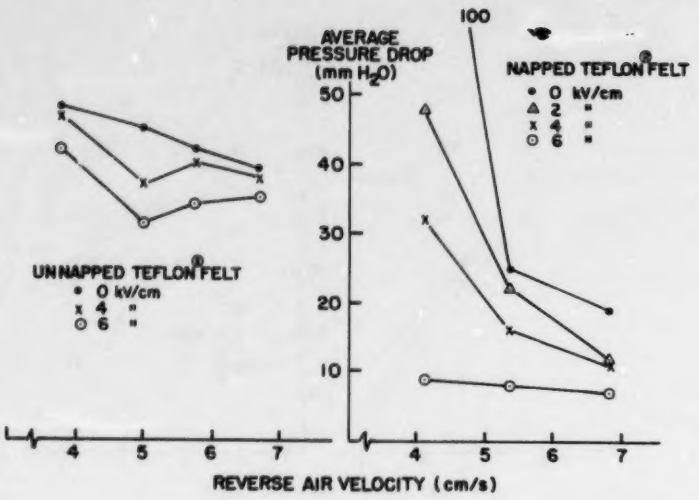

Figure 16. Averages of initial and final pressure drops, $(\Delta P_f - \Delta P_i)/2$, for unnapped and napped Teflon® felts.

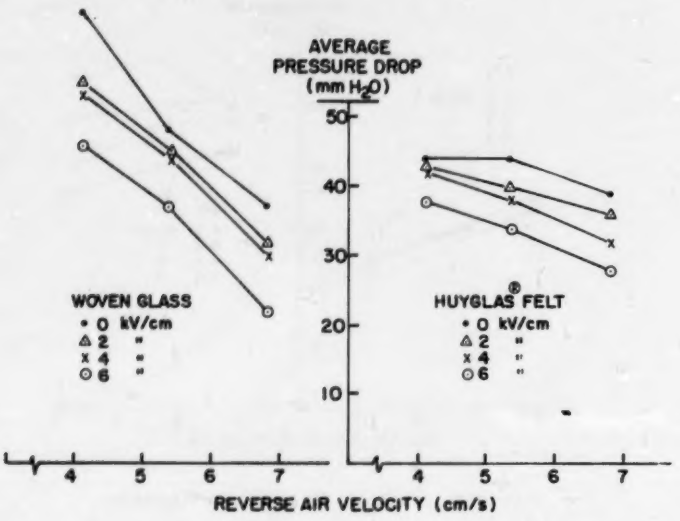

Figure 17. Like Figure 16, for type 648 woven glass fabric and Huyglas® glass felt.

thus proportional to the energy consumption associated with each set of conditions. The greater response of energy consumption in the case of the napped Teflon® felt to both ESFF and cleaning vigor is again illustrated.

To summarize these results, the napped Teflon® felt showed the strongest responses to both applied field and to reverse-air velocity. The response is sufficiently strong so that, if the filter is cleaned sufficiently well, substantial reductions in pressure drop may be obtained by virtue of the nap alone, even without application of ESFF. This felt also showed a strong reduction in ΔP_t with applied voltage at the lowest reverse-air velocity, but this dependence quickly disappeared as the fabric was cleaned more efficiently. The woven glass fabric showed the next strongest response to cleaning vigor and to applied field. On the other hand, the Teflon® and glass felts showed essentialiy no response of ΔP_t to applied field, i.e., the applied field did not aid in the cleaning process. This result appears to contradict earlier findings, in which Teflon® felt fabric gave lower PDR values than woven glass. However, those earlier results, unlike the recent ones, were obtained with the fabrics being cleaned by pulse-jet, which suggests that pulsing cleans more thoroughly. Measurements like those reported here should be repeated with the apparatus set up to clean with a pulse.

SECTION 7

CHARGE ELIMINATION IN LOBED-FIBER FILTERS BY METAL COATING

A series of experiments was conducted to investigate further the previously suggested hypothesis (Miller *et al.*, 1979) that electrostatic effects are at least partially responsible for the better performance obtained with trilobal in comparison with round-fiber filters. The purpose of the experiment was to clarify whether the principles underlying this improved performance were purely mechanical or whether they were also electrostatic. The reduced penetration through trilobal fiber filters may be explained on mechanical grounds by consideration of the larger effective diameters of trilobal fibers or on an electrostatic basis by assuming the presence of localized fields in the filters due to charges on fibers and particles. Of course, both mechanisms may contribute. The reduced pressure drop with trilobal fiber filters is not as easily explained, but has been empirically shown (Miller *et al.*, 1979) to be associated with cake formation closer to the upstream surface resulting in easier cake removal.

The first experiment set up in an attempt to clarify the principles involved used four patch filters, two of which had a gold coating vacuum-deposited on the filtering surface. The four samples included trilobal and round-fiber filters (3-den polyester, needled, 0.5 kg/m^2). To see whether the coating increased the effective conductance of the fabric, a voltage was applied from one edge of the patch to the other. The gold deposits increased the current through each patch by a factor of 10^3 (from 10^{-8} to 10^{-5}A at 1 kV). If buildup of charges on the filters is responsible for filtration performance differences, these differences would disappear for the gold-coated filters. Flyash filtration was carried out with no external field applied, so that the only electrical effects were due to the charges carried to the filter by the particles. Face velocity was 0.06 m/s (12 ft/min), and inlet concentration was 3.3 g/m^3. After fifty cycles of 5-min duration, performance had stabilized for each of the four filters. The steady-state values for penetration, pressure drop rise, and residual cake mass after cleaning are given in Table 2.

TABLE 2. FILTRATION PERFORMANCE OF GOLD-COATED POLYESTER FILTER FABRICS AFTER 50 CYCLES OF CONDITIONING

	Penetration (%)	Pressure drop rise (mm H_2O)	Residual cake after cleaning (% of filter mass)
Round (control)	<0.1	145	122
Round (gold-coated)	<0.1	145	102
Trilobal (control)	<0.1	115	75
Trilobal (gold-coated)	<0.1	142	104

Mass penetration values for all four samples were below 0.1%, so that differences were not detectable under these conditions. However, a significant decrease in pressure drop rise was obtained only with the nonconducting trilobal fiber filter (as found in previous measurements). There was no difference in pressure drop between the trilobal and the round samples that were made conductive. It appears, therefore, that electrostatic charges are largely responsible for pressure drop reduction with trilobal fiber filters. It can also be seen that the lower pressure drop rise is associated with a lower mass of residual cake after cleaning (expressed as a percentage of the mass of the filter). This is consistent with previous findings.

Penetration with the four needled polyester filters was so low that it was impossible to detect differences between samples with the equipment used. The same kind of measurement was repeated, therefore, with bonded nylon felts which, being lighter in weight (0.24 kg/m^2), would allow greater penetration. Nylon fibers were chosen for this new set of samples, not to examine the effect of different polymeric composition, but because they were available in three lobe depths, AR = 1.0, 1.5, and 2.2. Variations in lobe depth are characterized by the aspect ratio, AR. This is the ratio of the diameters of the circumscribed to the inscribed circles as shown in Figure 18 along with cross sections of the nylon fibers. Measurements of penetration, pressure drop, and residual cake mass were made between 10 and 20 filtering/cleaning cycles and then again between 25 and 35 cycles. Conditions for filtration were as follows: face velocity, 6 cm/s; inlet concentration of flyash, 6 g/m^3; cycle time, 5 min. Considering the results for uncoated filters given in Figure 19 (lower curves) and Table 3, it can be seen that penetration for the filter with lobe depth parameter AR = 2.2 is about 50% less than that with round fibers. This agrees with findings obtained previously with trilobal polyester fibers with an AR of ~2.1 (Miller *et al.*, 1977). It can also be seen that the shallow-lobed fiber filter (AR = 1.5) is only slightly lower in penetration than the round-fiber filter.

Pressure drop rise (Table 3) remains about the same for all three filters. This does not agree with data obtained for the polyester needled filters, which indicated that pressure drop is lower with fibers of AR = 2.2 than with round fibers. The discrepancy may be due to the differences in packing density of the surface fibers of the two types of filter. The Vinyon-bonded nylon samples have noticeably denser surface layers than the needled polyester samples, although this difference is difficult to measure quantitatively.

Turning now to examination of the samples coated with gold, the conductivity of the filters was checked to ensure that the coating had indeed brought about an increase. An estimate of the change in conductivity induced by the coating was made by measuring the current passed by the fabric when a 1-kV potential difference was applied across it, from one edge to the other. With the needled samples, an increase in current by a factor of 1000 was measured. With the three nylon samples, it was found that the resistance of the fabric had been lowered so much that the power supply could not deliver enough current to maintain the 1-kV potential difference across it. It is believed that the higher packing density of the surface layers of these nonwovens produces a more concentrated and, therefore, more conductive gold coating.

The results for the gold-coated fabrics in Figure 19 (upper curves) and Table 3 show that the sample with AR = 2.2 no longer reduces penetration by 50%. Penetration for this sample is equal to that for the other samples (about 1%) from the 10th to the 20th cycle. At this lighter weight (0.24 kg/m^2) penetration levels are fairly high, and differences due to a gold coating can now be detected. Between cycles 10 and 20 pressure drop and residual cake mass are not consistently affected by gold-coating. Between 25 and 35 cycles a catastrophic change occurs in every gold-coated sample. Penetration increases from 1% to over 10%. This increase is accompanied by a significant increase in residual cake mass. It appears, therefore, that with elimination of all charge, upstream capture does not occur, particles penetrate deeply, and efficiency is adversely affected. This effect apparently occurs for round-fiber filters as well as for trilobal.

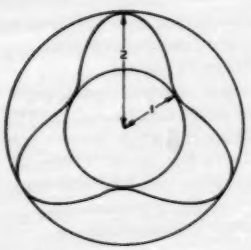

Cross section of fibe.
with aspect ratio 2.

Figure 18. Cross-sectional views of three DuPont nylon fibers. Top to bottom: round (AR = 1.0), shallow-lobed trilobal (AR = 1.5), and deep-lobed trilobal (AR = 2.2).

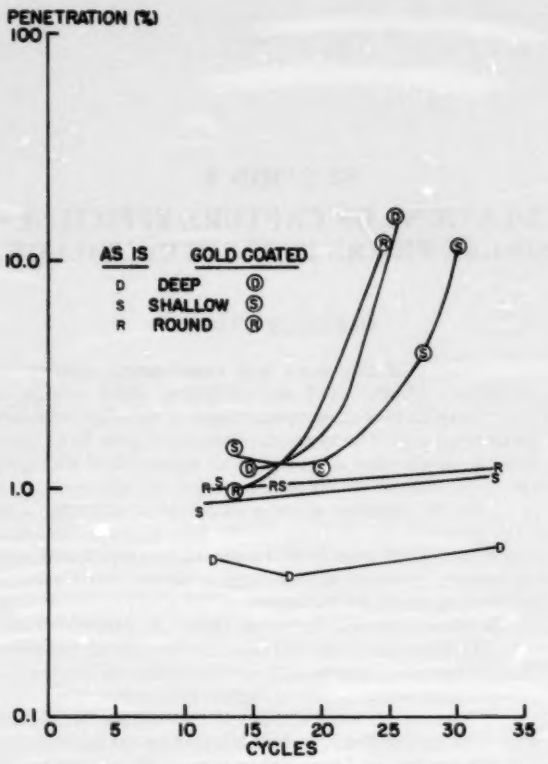

Figure 19. Penetration of flyash as filtering progresses through fabrics made of the fibers in Figure 18 (R, S, and D, respectively), and through these fabrics after vacuum deposition of gold (Ⓡ, Ⓢ, and Ⓓ).

TABLE 3. EFFECTS OF LOBE DEPTH AND CHARGE ELIMINATION

	Uncoated			Gold-coated		
	Trilobal		Round	Trilobal		Round
10-20 cycles	AR=2.2	AR=1.5	AR=1	AR=2.2	AR=1.5	AR=1
Penetration (%)	0.5	1.0	1.0	1.2	1.3	1.0
($\Delta P_f - \Delta P_i$) (mm H_2O)	89	85	89	94	60	90
% Residual cake	96	106	91	96	100	103
25-35 cycles						
% (1 - E)	0.6	1.1	1.3	16.3	12.0	12.2
($\Delta P_f - \Delta P_i$) (mm H_2O)	89	83	89	100	75	82
% Residual cake	121	112	124	141	143	152

SECTION 8

CALCULATIONS OF CAPTURE EFFICIENCY OF SINGLE FIBERS IN ELECTRIC FIELDS

INTRODUCTION

The original objective of this work was experimental verification of some theoretical predictions (Zebel, 1965 and O'Meara, 1979) relating single-fiber efficiencies in electric fields to cross-sectional shape of the fiber and the strength and direction of the external field. The apparatus shown in Figure 20 was constructed to bombard a fiber or simple fiber assembly in an electric field with particles in an aerosol stream. The method of measurement was to remove the target fiber, photograph it under the scanning electron microscope, and then make particle counts from the photographs. It immediately became apparent that under the experimental conditions used, large dendritic structures were formed, and this raised the question of how the presence of these large structures might affect the capture efficiency. This, in turn, could not be verified unless effective means were found for examining the dendrites without breaking them. A procedure for obtaining photographs of undamaged dendrites was therefore developed, but before the main objective of the investigation could be addressed, a further difficulty arose. This was the unusually large scatter of the measured capture efficiencies. The cause was traced to the strong dependence of efficiency on fiber orientation and location with respect to the electrodes. This section describes how this finding has led to the examination of potential-induced charges on fibers and to their effect on capture efficiency.

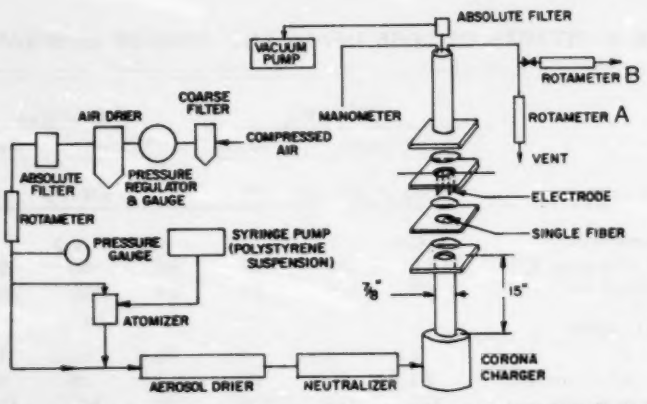

Figure 20. Schlematic diagram of apparatus for studying particle capture by a single fiber.

FORMATION OF DENDRITES

Initial experiments were performed to examine the structures formed by the particles collected on single fibers in an electric field. A round polyester filament 16 μm in diameter was used; the particles were polystyrene spheres 1.2 μm in diameter. The fiber was located midway between two electrodes (position 2 in Figure 21). The exact location was not measured precisely until its importance was recognized as explained below.

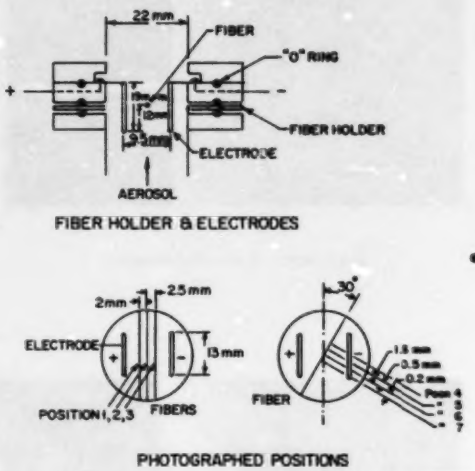

Figure 21. Fiber positions corresponding to Figures 22 and 24.

The photographs in Figure 22 were taken through an electron microscope after the samples had been gold-coated. The dendritic structure was sometimes disrupted by strong electric fields in the coating procedure, by electron beams in the microscope, or by atmospheric disturbances. To minimize the disruption of dendrites, the fiber sample was covered by a metal plate with a slit, and the sample was gold-coated and photographed through this aperture. In addition, the lowest voltages of the gold coater and of the microscope were used.

Figure 22 shows clearly the uneven distribution of particles and dendrites. As the dendrites grow, later particles are captured on the ends, and consequently the dendrites may play an important role in particle capture by the fiber and in the way that the collection efficiency depends on the number of particles already deposited. Moreover, the experimental collection efficiencies for clean fibers failed to agree with the theoretical computations. It was therefore decided to re-examine particle capture on clean single fibers.

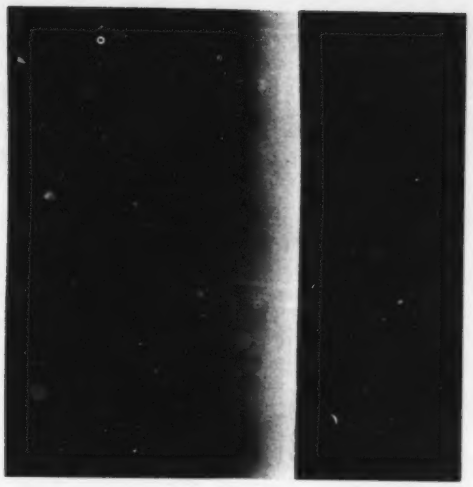

Run time: 5 min (upstream)

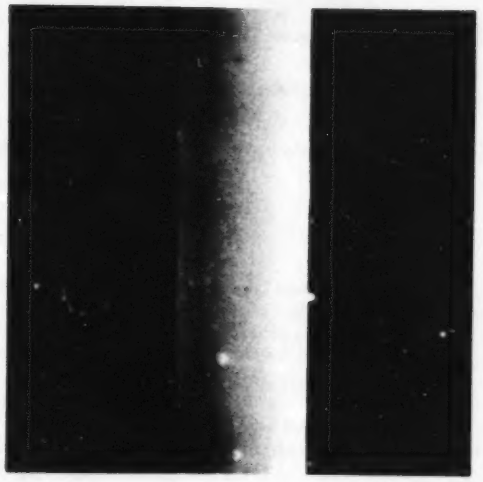

Run time: 5 min (downstream)

Figure 22. Dendrite growth on upstream and downstream sides of fiber after filtration for times indicated. Fiber at position 2 (Fig. 19); V_0=34 cm/s; E_0=5.3 kV/cm; aerosol concentration 600 particles/cm^3.

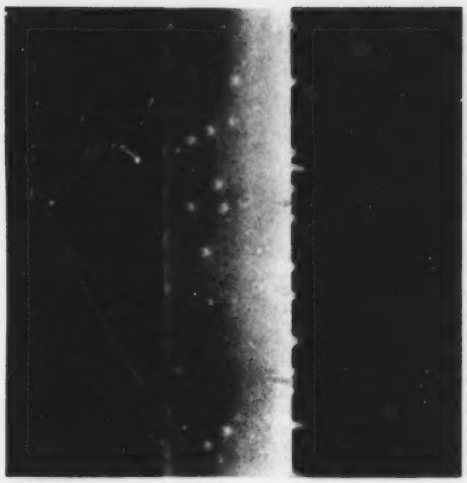

Run time: 20 min (upstream)

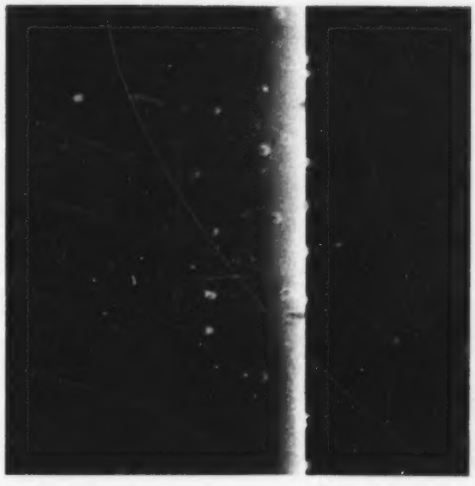

Run time: 20 min (downstream)

Figure 22. Dendrite growth (continued).

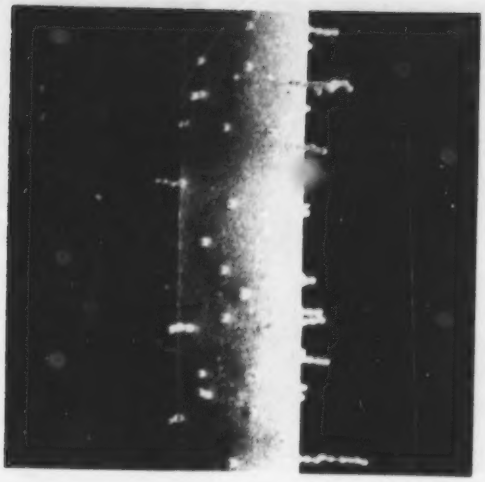

Run time: 30 min (upstream)

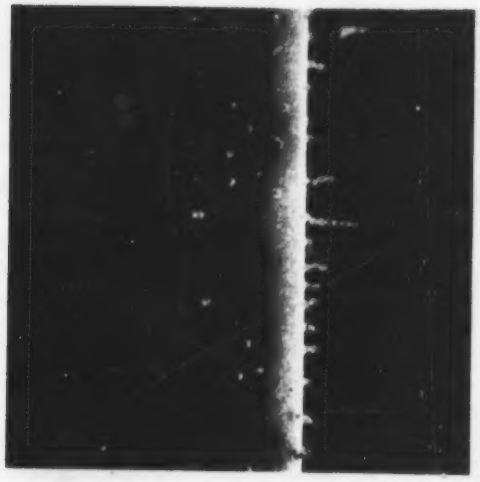

Run time: 30 min (downstream)

Figure 22. Dendrite growth (continued).

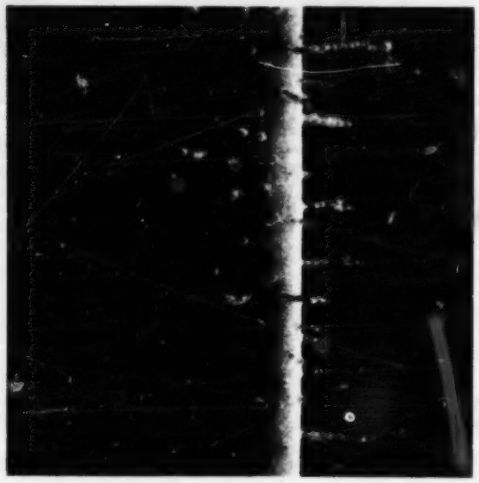

Run time: 60 min (upstream)

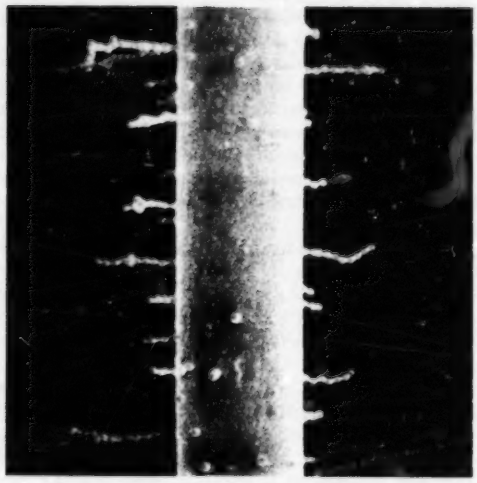

Run time: 60 min (downstream)

Figure 22. Dendrite growth (continued).

COLLECTION EFFICIENCY OF SINGLE FIBERS (EXPERIMENTS WITH UNCHARGED PARTICLES)

One measure of effectiveness for a single fiber is the collection efficiency, η, which is simply the upstream area from which particles are captured divided by the projected area of the collector. According to Zebel's theory for uncharged particles (Zebel, 1965), η is determined by three parameters: the Reynolds number, Re, which sometimes appears in the form $f = 2 - \ln Re$; a parameter F involving the ratio of electrical to viscous forces on the particle, where:

$$F = 2\left[\frac{\epsilon_p^{-1}}{\epsilon_p^{+2}}\right]\left[\frac{R_p^3}{R_c}\right]\frac{aE_0^2B}{V_0} \qquad [1]$$

and another, a, involving the electrical properties of the collector and the surrounding fluid, given by:

$$a = \frac{\epsilon_c^{-1}}{\epsilon_c^{+1}} \qquad [2]$$

where ϵ_p, ϵ_c = the dielectric constants of the particle and the fiber, R_p, R_c = radii of the particle and the fiber, B = mobility of the particle, E_0 = external electric field intensity, and V_0 = air velocity.

In order to test the theory, collection efficiencies were measured at various electric fields E_0 and aerosol velocities V_0. The experimental results are summarized in Table 4. The running time of the experiments was fixed at one hour without considering the effects of dendrites. Thus, the number of particles captured by the fiber was not constant, but the dendrite formation was negligible when the number of deposited particles (Table 4) was less than about 100. The fiber in each experiment was located midway between the two electrodes (position 2 in Figure 21) except in experiments 12 and 13. These two experiments were specially designed to trace the cause of scattering in the experimental data seen in Figure 23. In experiment 12, the fiber was positioned off-center (position 3 in Figure 21). In experiment 13 three fibers were installed on the same fiber holder; experiments 13-1, 13-2, and 13-3 represent the results for the fibers in positions 2, 3, and 1 in Figure 21, respectively. The aerosol velocity V_0 is calculated with the assumption of fully-developed laminar flow, that is, V_0 is twice the average velocity when the fiber is located at the center. The aerosol concentrations except in experiments 7 to 15 were the average mass of particles collected in six runs.

The measured collection efficiencies η are plotted as function of F, the ratio of electric to drag forces, in Figure 23. Although in calculating F we assume that the fiber and the particles are conductors (a = 1), theoretical calculations at other conditions are also plotted. For comparison, Kirsch's (Kirsch, A., 1972) experimental results are plotted as well (curve 4).

The following observations can be made about the experimental results:

(1) The experimental collection efficiencies are much higher than the theoretical ones.

(2) An electric field oriented perpendicular to the fiber and to the flow direction sets up repulsive forces on the sides of the fiber facing up and downstream.

TABLE 4. SINGLE-FIBER CAPTURE EFFICIENCY UNDER DIFFERENT EXPERIMENTAL CONDITIONS

Exp. no.	V_0 (cm/s)	E_0 (kV/cm)	Aerosol conc. (no. particles/ cm³	No. particles deposited per 120-μm length of fiber	Collec. Effic. η
1	8.9	0	470	9	0.031
2	8.9	1.1	470	12	0.042
3	8.9	2.1	470	17	0.059
4	8.9	3.2	470	42	0.15
5	8.9	4.2	470	165	0.57
6	8.9	5.3	470	73	0.25
7	18	0	1510	9	0.0049
8	18	1.1	1190	21	0.015
9	18	3.2	970	39	0.040
10	18	4.2	1350	133	0.081
11	18	5.3	1110	140	0.10
12	16	5.3	1030	299 (per 60 μm)	0.52
13-1	18	5.3	1110	75 (per 60μm)	0.11
13-2	17	5.3	1110	487 (per 60 μm)	0.74
13-3	17	5.3	1110	400 (per 60 μm)	0.63
14	23	0	410	6	0.009
15	23	1.1	410	10	0.016
16	23	2.1	410	66	0.10
17	23	3.2	410	10	0.016
18	23	4.2	410	87	0.14
19	23	5.3	410	40	0.062
20	34	0	290	4	0.0059
21	34	1.1	290	5	0.0074
22	34	2.1	290	20	0.030
23	34	3.2	290	39	0.058
24	34	4.2	290	245	0.36
25	34	5.3	600	534	0.37

Thus in Figure 22 there should be particle-free bands running down the center of the fibers. In spite of these forces, particles are seen to be captured near the centers.

(3) Data points are scattered.

It is appropriate at this point to give details of the experimental procedure that might be suspected to give rise to some of the anomalies in the results. Figure 20 shows that the air flow system was of the push-pull type, having a vacuum pump at the downstream end, and being supplied with compressed air at the upstream end. Thus, as the absolute filter collected particles and the pressure difference increased, the flow through the vacuum pump was adjusted so as to maintain atmospheric pressure in the sample tube. This adjustment was made possible by the flow meter (rotameter) A which had a capacity much less than 1% of that of rotameter B. At the

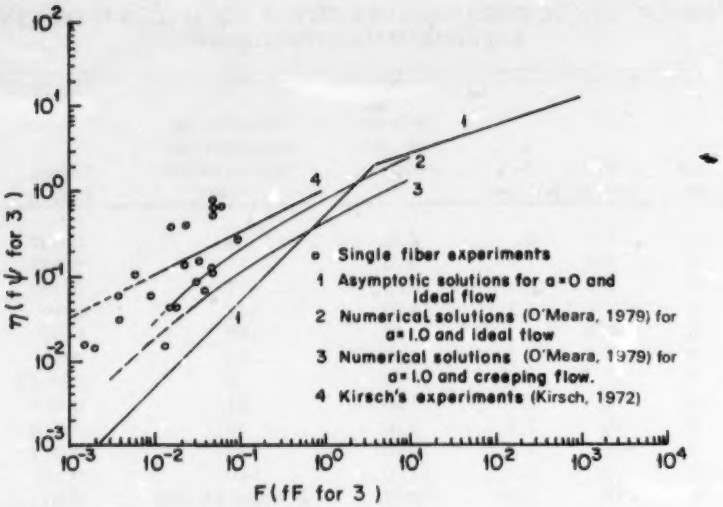
η(fψ for 3)
F(fF for 3)
Single fiber experiments
1 Asymptotic solutions for a=0 and ideal flow
2 Numerical solutions (O'Meara, 1979) for a=1.0 and ideal flow
3 Numerical solutions (O'Meara, 1979) for a=1.0 and creeping flow.
4 Kirsch's experiments (Kirsch, 1972)

Figure 23. Comparison of measured capture efficiencies (single-fiber experiments) with calculated values.

beginning of an experiment, the vacuum pump was off and flow was adjusted using B. This measurement was also a check on leaks in the system, since at a given compressed air pressure, the flow through the atomizer nozzle was constant. After this, the vacuum pump was turned on and its flow adjusted until B read zero. The valve to B was then closed and thereafter the flow to the pump was adjusted so as to maintain a small reading on A. The small loss of aerosol through A was considered negligible. This system is believed to give well-controlled flow and should not be the cause of erratic results. Another source of scatter in the results could have been variations in the inlet concentration. The extent of this can be judged from the results in Table 4. For experiments 1–6, 14–19, and 20–24, the reported concentration was obtained by collecting particles over all 5 or 6 runs in the group and calculating the average. This was necessary because of the small mass of particles collected in one experiment. In runs 7–13 the concentration was higher, and the particles collected in each run were weighed. This allows an estimate of the variation, which is seen to amount to about 25%. It must be remembered that even in runs 7–13 the amount collected was small and some error in weighing was to be expected. For this reason, the averaged values should be more reliable. In any case, it is important to note that the measured variations in inlet concentration were 25%, while measured variations in efficiency were about 1000%.

Experiments 12 and 13 show that the collection efficiency depends strongly on the location of the fiber. The collection efficiencies of the off-centered fibers (experiments 12, 13-2, and 13-3) are about five times higher than those of the centered fibers (experiments 11 and 13-1) at the same electric field and velocity.

In order to determine the width of the low collection region of the apparatus the fiber was rotated 30° as shown in Figure 21. The results are pictured in Figure 24. Within 1 mm of the centerline parallel to the electrodes, very few particles were captured, as shown in the pictures of positions 5, 6, and 7. But many particles were captured off this narrow region as shown in the picture of position 4. Consequently, small differences in the fiber positions could account for scatter in the data and cause the other two unexpected observations as well. Zebel's theory, however, does not predict any effect of fiber location on collection efficiency.

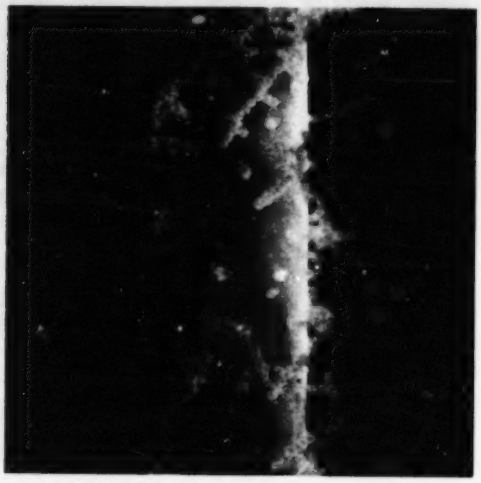

Position 4

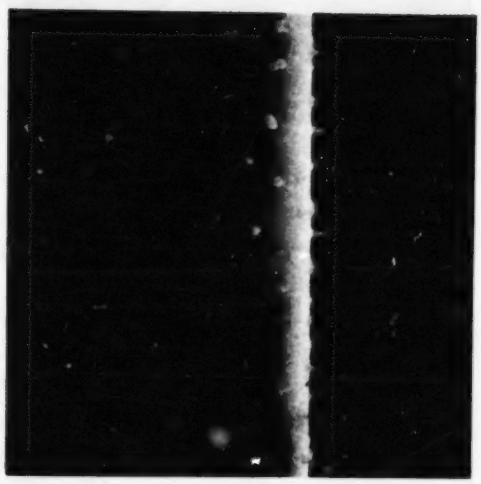

Position 5

Figure 24. Particle capture at different locations of fiber tilted 30° from normal position (See Fig. 21).

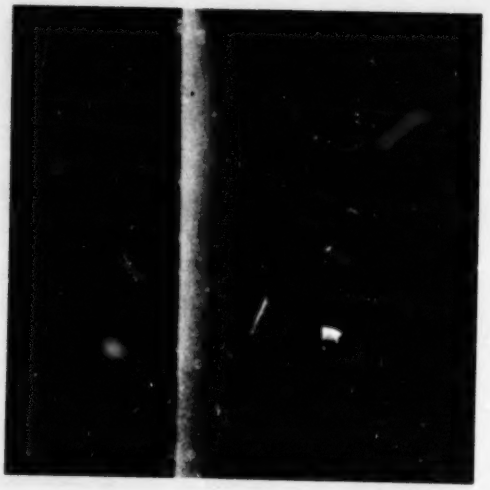

Position 6

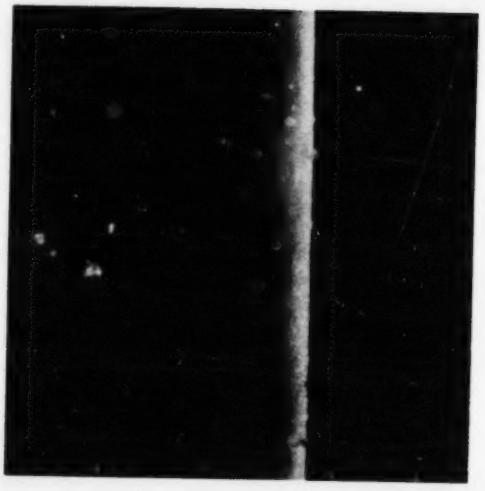

Position 7

Figure 24. Particle capture (continued).

POTENTIAL-INDUCED CHARGE IN A UNIFORM EXTERNAL FIELD

A theoretical treatment was now developed to explain the experimental observation that particle capture by a single fiber depends strongly on its location between two electrodes. In the theory this geometric effect is represented by a parameter A (refer to Eq. 7), which is obtained for the case of a grounded fiber between two plate electrodes. The theory predicts that an external field induces a net charge on the fiber, the magnitude depending on the value of A. It also predicts that the geometric effect can overwhelm the effect of the dipole moment. The theoretical calculations are in good agreement with the experimental results. Furthermore, the discrepancy between Zebel's theory and experimental results (Zebel, 1965 and Kirsch, 1972) may be clarified by including the geometric parameter A.

We consider the electric field near a grounded conductive fiber between two plate electrodes as shown in Figure 25. This is probably the simplest experimental geometry for testing the theories. The distance between the two electrodes is 2b and the fiber radius R_c. The fiber is displaced from the centerline between the two electrodes by the distance d. The electric potential ψ of the external field at the centerline and that of the fiber (ground) are both taken to be zero.

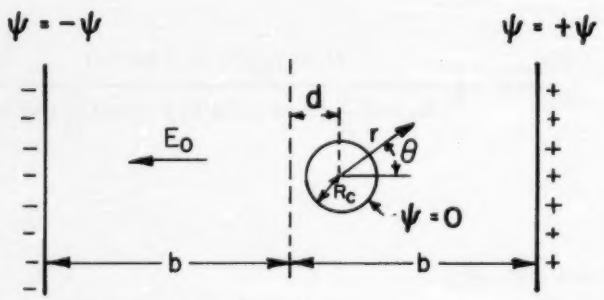

Figure 25. Geometry of an off-center fiber between two plate electrodes.

Then, from Maxwell's equations of electromagnetic theory, the electric potential ψ in cylindrical coordinates can be written:

$$\frac{1}{r}\frac{\delta}{\delta r}\left(r\frac{\delta\psi}{\delta r}\right)+\frac{1}{r^2}\frac{\delta^2\psi}{\delta\theta^2}=0 \qquad [3]$$

with the boundary conditions

(1) $\psi = 0$ at r = 1,

(2) $\psi = \psi_0$ at r cos θ = b–d,

(3) $\psi = -\psi_0$ at cos θ = –b–d,

where unit length = R_c and (b–d) >> 1.

Taking into account that the boundary conditions involve both cylindrical and rectangular properties, two solutions for ψ are proposed, one near the fiber (inner solution) and one near the electrodes (outer solution). The inner solution may be obtained by applying the method of separation of variables with the boundary condition at the fiber surface:

$$\psi = C_1 \ln r + C_2 (r - \frac{1}{r}) \cos \theta. \qquad [4]$$

Since the interaction between the fiber and the electrodes is negligible for $(b-d) >> 1$, higher order terms are discarded in the above equation. The first term represents a line charge at the center of the fiber. The second and third terms are the uniform field and the dipole moment of the fiber, respectively. The constants C_1 and C_2 will be determined by matching to the outer solution. Because the potential of the dipole moment rapidly fades out as r becomes large, the outer solution is defined as the electric field for a line charge q between two plate electrodes. The charge q will also be determined from the matching of the inner and outer solutions. Using the Schwarz transformation, the outer solution can be written (Smythe, 1968):

$$\psi = E_0 R_c r \cos \theta + E_0 R_c d \qquad [5]$$

$$+ \frac{8}{2\pi\epsilon} \tanh^{-1} + \left\{ \frac{D_1 \sin [\frac{\pi}{2b}(b - d - r \cos \theta)]}{-D_2 \cos [\frac{\pi}{2b}(b - d - r \cos \theta)] + \cosh [\frac{\pi}{2b} r \sin \theta]} \right\},$$

where

$D_1 = \sin [\frac{\pi}{2b}(b - d)]$,

$D_2 = \cos [\frac{\pi}{2b}(b - d)]$,

E_0 = external field intensity ψ_0 / bR_c,

and ϵ = the dielectric constant of air.

For $d << b$, this potential can be approximated as:

$$\psi = E_0 R_c r \cos \theta + E_0 R_c d + \frac{q}{2\pi\epsilon} \ln (\frac{4b}{\pi r}). \qquad [6]$$

Now the constants in Equation 4 can be determined from this outer solution. By matching Equations 4 and 6 at $1 \ll r \ll (b-d)$, the electric field around the fiber can be described as:

$$\psi = AE_0R_c \ln r + E_0R_c\left(r - \frac{1}{r}\right)\cos\theta, \qquad [7]$$

where $A = d/R_c \ln\left(\frac{4b}{\pi R_c}\right)$.

The parameter A represents the potential-induced charge. The potential difference, E_0R_cd, between the fiber and the external field at the fiber center induces a net charge on the fiber. If the fiber is centered exactly between the two electrodes, d = 0, and the external field induces only a dipole moment on it. However, by displacement of the fiber from the centerline, a net charge can be induced on the fiber. The charge depends on the distance between the electrodes 2b as well as on d. It should be noticed that because of the logarithmic relation in A, the charge is not negligible even when d is much smaller than b.

COLLECTION EFFICIENCY FOR FIBERS WITH POTENTIAL-INDUCED CHARGES (UNCHARGED PARTICLES)

The electric force $\overline{K}$, on an uncharged spherical particle with radius R_p and dielectric constant ϵ_p, is:

$$\overline{K} = \frac{R_p^3}{2}\left[\frac{\epsilon_p - 1}{\epsilon_p + 2}\right]\nabla(-\nabla\psi)^2. \qquad [8]$$

A simple calculation shows that Equation 8 is a good approximation except very near the fiber surface. Applying Equation 7 gives the radial and tangential components of the electric force, K_r and K_θ:

$$K_r = -2\left[\frac{\epsilon_p - 1}{\epsilon_p + 2}\right]\left[\frac{R_p^3}{R_c}\right]E_0^2\left[\frac{A^2}{2}\frac{1}{r^3} + \frac{A}{2}\left(\frac{1}{r^2} + \frac{3}{r^4}\right)\cos\theta\right.$$

$$\left. + \left(\frac{1}{r^3} + \frac{1}{r^3}\cos 2\theta\right)\right], \text{ and} \qquad [9a]$$

$$K_\theta = -2\left[\frac{\epsilon_p - 1}{\epsilon_p + 2}\right]\left[\frac{R_p^3}{R_c}\right]E_0^2\left[\frac{A}{2}\left(\frac{1}{r^2} + \frac{1}{r^4}\right)\sin\theta + \frac{1}{r^3}\sin 2\theta\right]. \qquad [9b]$$

In establishing the differential equations for the particle trajectories, gravity and inertia of the particles are neglected as usual. In calculations of drag forces, Stokes flows are assumed both for the particle and the fiber. In the experiments, the Reynolds number of the fiber is less than one. With these assumptions, the differential equations of the particle trajectories when the air flow is perpendicular to the electric field can be written:

$$\frac{dr}{dt} = -\widetilde{F}\left[\frac{A^2}{2}\frac{1}{r^3} + \frac{A}{2}\left(\frac{1}{r^2} + \frac{3}{r^4}\right)\cos\theta + \left(\frac{1}{r^5} + \frac{1}{r^3}\cos 2\theta\right)\right]$$

$$+ 0.5\left[2\ln r - \left(1 - \frac{1}{r^2}\right)\right]\sin\theta, \text{ and} \qquad [10a]$$

$$\frac{r\,d\theta}{dt} = -\widetilde{F}\left[\frac{A}{2}\left(\frac{1}{r^2} + \frac{1}{r^4}\right)\sin\theta + \frac{1}{r^3}\sin 2\theta\right]$$

$$+ 0.5\left[2\ln r + \left(1 - \frac{1}{r^2}\right)\right]\cos\theta, \qquad [10b]$$

where $\widetilde{F} = fF = f\left(\frac{\varepsilon_p^{-1}}{\varepsilon_p + 2}\right)\left(\frac{R_p^2}{R_c}\right)\frac{E_0^2}{3\pi\mu V_0}$; μ = the air viscosity;

and B (Eq. 1) = $1/6\pi\mu R_p$.

Using Equations 10a and 10b, particle trajectories and collection efficiencies, η, were obtained numerically for various values of $\widetilde{F}$ (a function of external field intensity, E_0) over a range of values of A. The calculated efficiencies are plotted as a function of $\widetilde{F}$ in Figure 26. As A increases, the efficiency increases but the slope of the efficiency curve decreases slightly, so that the effect of the induced charge is a little greater at small values of $\widetilde{F}$. In addition, since the slope is less than one, the efficiency decreases as Reynolds number decreases or as f (2 − ln Re) increases at a constant $\widetilde{F}$. Figure 26 indicates that Zebel's theory (A = 0) predicts only the minimum η. Thus, experimental results higher than Zebel's predictions (e.g., Fig. 23) may be explained by including the potential-induced charges on the fiber.

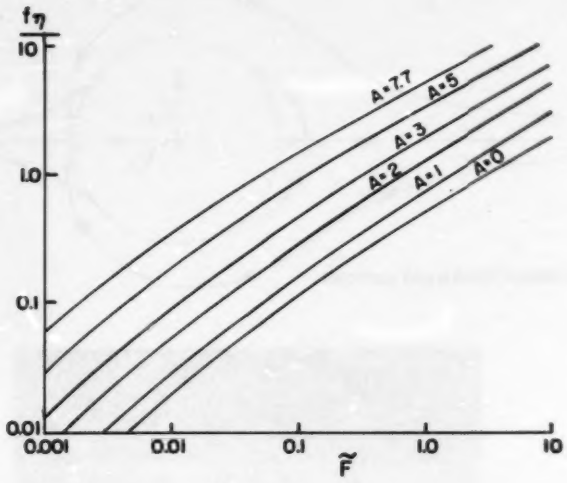

Figure 26. Collection efficiencies for uncharged particles on fibers with potential-induced charges.

COMPARISON WITH EXPERIMENTAL RESULTS

The scanning electron micrographs (SEMs) in Figures 27–30 are presented here for comparison with the theoretical calculations for four values of d (that is, of A) at a constant $\tilde{F}$. Uncharged particles were used in these experiments. The experimental efficiencies, η_{ex}, were evaluated from the number of captured particles counted on the SEMs divided by the number of particles passing through the cross-sectional area of the fiber. The theoretical particle trajectories and collection efficiencies, η_{th}, were calculated numerically using Equations 10a and 10b. For these calculations, the fiber and particle were both assumed to be conductors. The conductivity of the fiber material used was high enough to allow the surface to become equipotential when an external electric field was applied. This was confirmed by experiments using gold-coated fibers; no difference was found between the collection efficiencies of these fibers and the uncoated polyester.

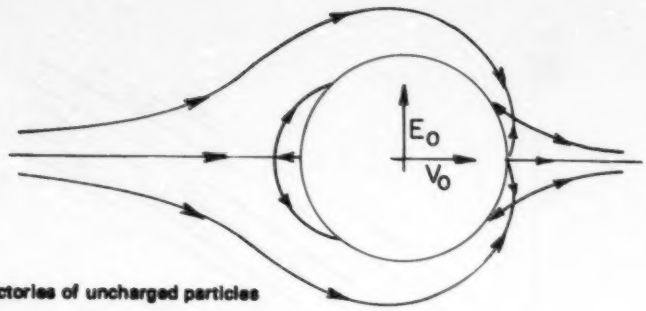

Trajectories of uncharged particles

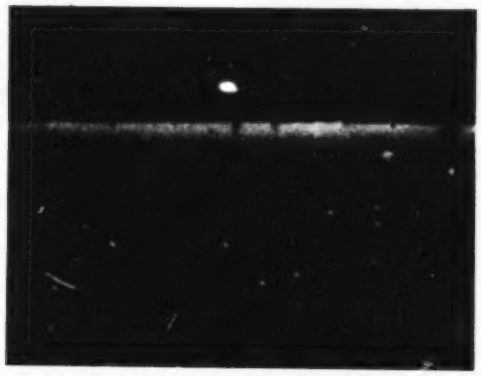

Upstream

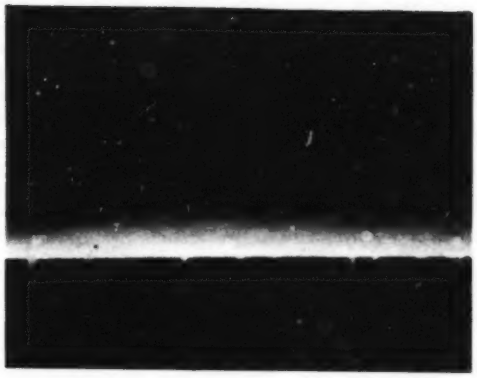

Downstream

Figure 27. Comparison of theory and experiment at d = 0.

Theoretical collection efficiency: η_{th} = 0.048

Experimental efficiency from SEMs: η_{ex} = 0.075

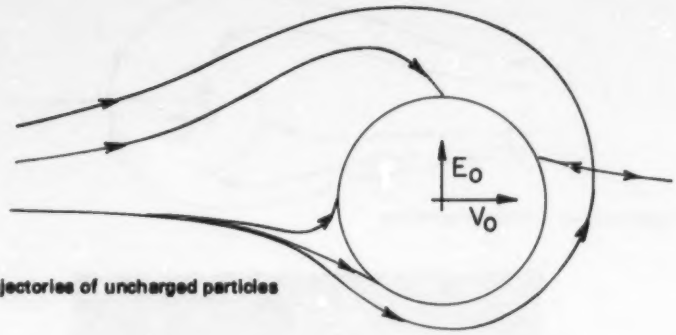

Trajectories of uncharged particles

Upstream

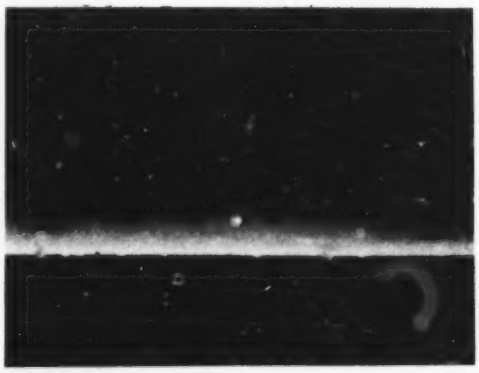

Downstream

Figure 28. Comparison of theory and experiment at d = 0.1 mm.

Theoretical collection efficiency: $\eta_{th} = 0.11$

Experimental efficiency from SEMs: $\eta_{ex} = 0.17$

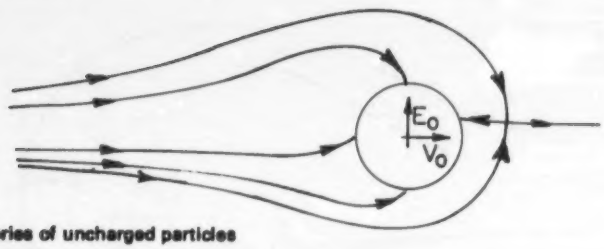

Trajectories of uncharged particles

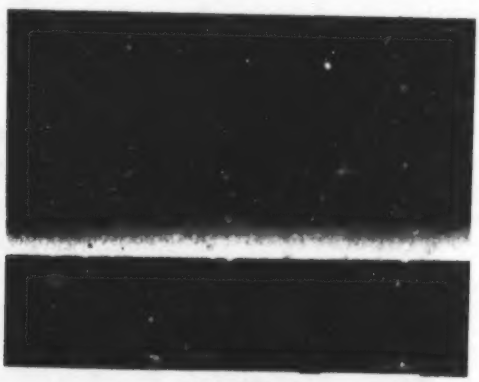

Upstream

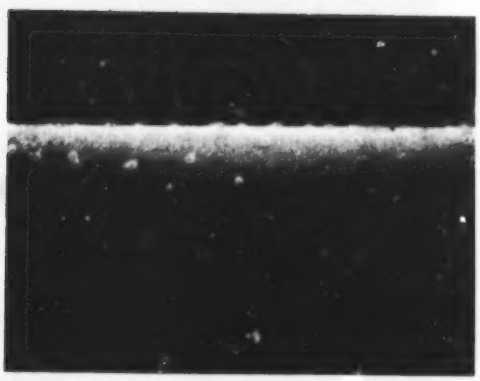

Downstream

Figure 29. Comparison of theory and experiment at d = -0.25 mm.

Theoretical collection efficiency: η_{th} = 0.33

Experimental efficiency from SEMs: η_{ex} = 0.18

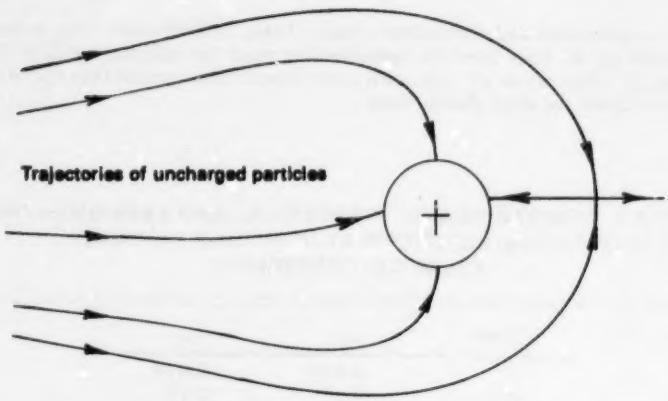

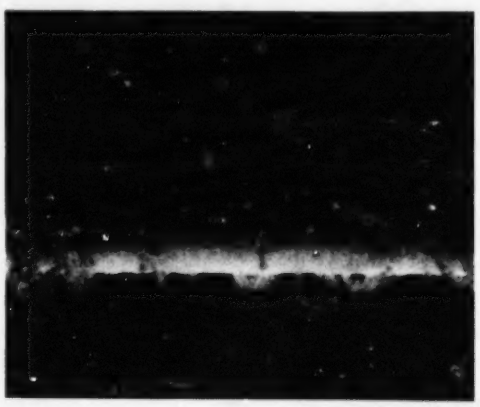

Upstream

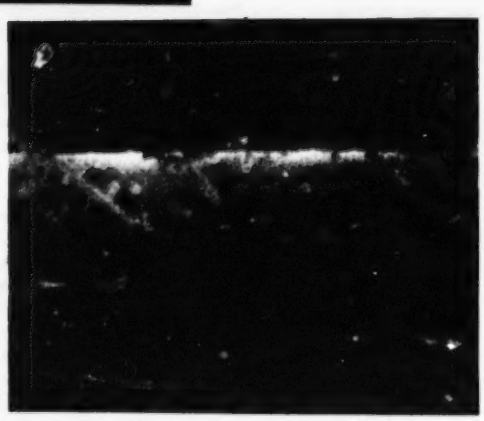

Downstream

Figure 30. Comparison of theory and experiment at d = -0.8 mm.

Theoretical collection efficiency: $\eta_{th} = 1.2$

Experimental efficiency from SEMs: $\eta_{ex} = 1.0$

The experimental and theoretical results (Table 5) both show that a small dislocation of the fiber from the centerline increases the efficiency greatly. For instance, the efficiency at d = −0.8 mm is more than ten times greater than that at the centerline under the same electric field.

TABLE 5. COMPARISON OF THEORETICAL AND EXPERIMENTAL COLLECTION EFFICIENCIES AT DIFFERENT DISTANCES d FROM THE CENTERLINE

d (mm)	η_{th}	η_{ex}
0	0.048	0.075
0.1	0.11	0.17
-0.25	0.33	0.18
-0.8	1.2	1.0

It is also noticeable that, depending on the value of d, particles are sometimes captured preferentially on one side of the fiber as shown in Figures 28 and 29. The calculated trajectories and the dendritic particle buildup in the SEMs both show clearly this asymmetric particle capture on the fiber. In order to compare the dendritic structures in the SEMs more clearly, lines of electric force for several values of A are shown in Figure 31. They were obtained numerically using Equations 9a and 9b. At A = 0, the external field induces equal numbers of positive and negative surface charges on the fiber, and the attractive and repulsive forces of the dipole moment are symmetric with respect to the fiber axis. As A increases, the net charge, positive or negative, increases the surface charge on one side of the fiber while it reduces that on the other side. At A = −2 the repulsive region disappears on the fiber and the particle capture becomes more clearly asymmetric.

However, the collection efficiency did not increase indefinitely with d. As d increased, the efficiency increased sharply but was saturated at a certain position. The result in Figure 30 was almost the maximum efficiency under the experimental conditions. It is likely that this limit occurs because the field intensity is limited by the corona discharge in the air. For instance, the field intensity on the fiber surface becomes >30 kV/cm at A = 7.7 under a 5.3-kV/cm external field. This is why the sharp change in particle capture was observed in a very narrow region near the centerline.

The theory and experimental results both indicate that geometric effects play a strong role in particle capture by fibers in external electric fields. This effect has not been recognized because in theoretical studies charged and uncharged fibers in an external electric field have been treated assuming isolated fibers. Because the fibers cannot be suspended in the air without any connection to solid bodies, however, this assumption is probably not applicable to electrified filtration.

In the present study, the geometric effect is represented by a parameter A, which is a function of the off-center distance d and the electrode separation 2b. Displacement of the fiber from the centerline results in differences between the potentials of the fiber surface and the external field. This difference in potential induces a net charge on the fiber. The amount of charge depends on both d and b. If A = 0, i.e., if the fiber is located exactly at the centerline, we may assume the fiber is uncharged, but this hardly ever happens, especially in the irregular geometry of a real fiber.

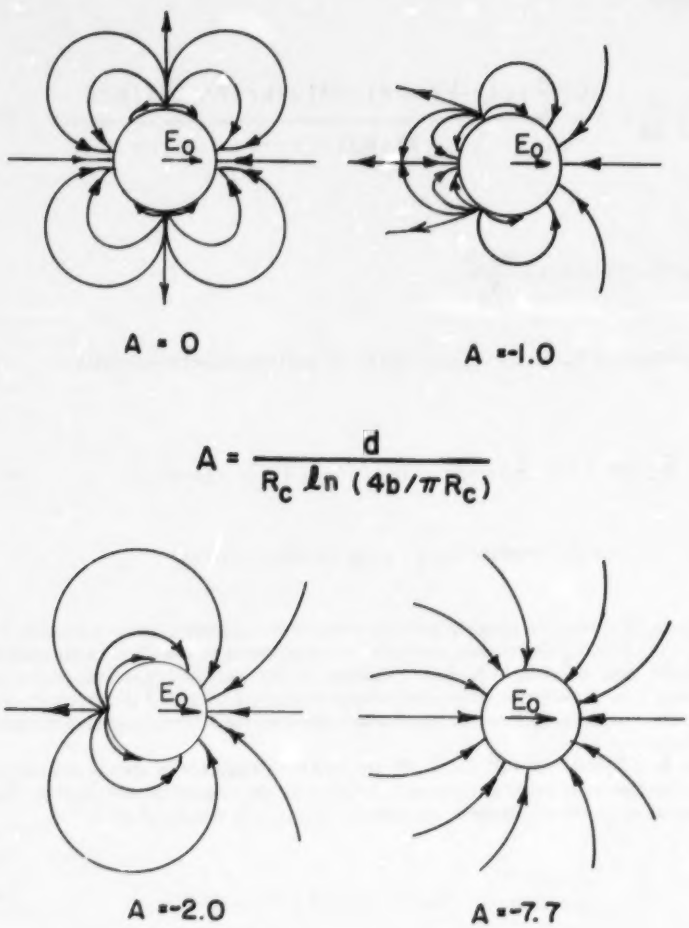

Figure 31. Lines of force for uncharged particles near fibers with potential-induced charges at several values of A.

COLLECTION EFFICIENCY FOR FIBERS WITH POTENTIAL-INDUCED CHARGES (CHARGED PARTICLES)

The electric force on a particle carrying an electric charge q_p is found by multiplying q_p by the electric field intensity $\vec{E}$. With the same assumptions used in deriving Equations 10a and 10b, the following differential equation is easily obtained:

$$\frac{1}{r}\frac{dr}{d\theta} = \frac{-\widetilde{G}\left[\frac{A}{r} + \left(1+\frac{1}{r^2}\right)\cos\theta\right] + 0.5\left[2\ln r - \left(1-\frac{1}{r^2}\right)\right]\sin\theta}{\widetilde{G}\left[\left(1-\frac{1}{r^2}\right)\sin\theta\right] + 0.5\left[2\ln r + \left(1-\frac{1}{r^2}\right)\right]\cos\theta}, \qquad [11]$$

where $\widetilde{G} = fG$, and $G = \frac{E_0 qB}{V_0}$.

The solution of the above equation gives the particle trajectory equation:

$$-\widetilde{G}\left[A\theta + r\left(1+\frac{1}{r^2}\right)\sin\theta\right] - 0.5r\left[2\ln r - \left(1-\frac{1}{r^2}\right)\right]\cos\theta \qquad [12]$$

$$= \psi_p \text{ (constant along a given particle trajectory).}$$

Figure 32 shows the limiting particle trajectories calculated using Equation 12. Within the limiting trajectories, all particles are captured by the fiber. In calculating the collection efficiency, Nielsen (Nielsen, 1978) classified particle collection behavior into three types which correspond to cases 1, 2, and 3 in Figure 32 and derived analytical solutions for cases 1 and 3. Here we extend his analysis to the three limiting cases.

For $A > 2$ (and $A > 1.45$ for $\widetilde{G} \to 0$), the two limit trajectories always meet at the same singular point as shown in case 3 in Figure 32. Because all terms except the first in Equation 12 are the same at the singular point, η is simply given by:

$$\eta = \pi GA \qquad \text{for } A \geq 2, \text{ and } A \geq \text{for } \widetilde{G} \to 0. \qquad [13]$$

For $A < 2$ and $\widetilde{G} \to \infty$, there is no singularity as shown in Figure 32, case 1, and the collection efficiency is:

$$\eta = G\left\{A\cos^{-1}\left(-\frac{A}{2}\right) + 2\left[1-\left(\frac{A}{2}\right)^2\right]^{1/2}\right\} \qquad \text{for } A<2 \text{ and } \widetilde{G}\to\infty. \qquad [14]$$

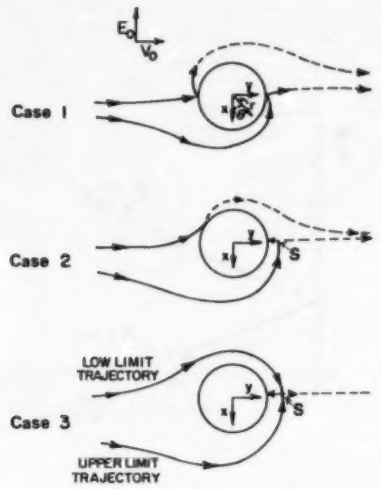

Figure 32. Limiting paticle trajectories for charged particles near a fiber with potential-induced charges.

Case 1 - no singular point ($A = 0$, $\widetilde{G} = 0.1$).

Case 2 - a singular point at S ($A = 1.0$, $\widetilde{G} = 0.1$).

Case 3 - a singular point at S ($A = 2.0$, $\widetilde{G} = 0.1$).

For $A < 1.45$ and $\widetilde{G} \to 0$, one limiting trajectory passes through a singular point (at $\theta = \frac{\pi}{2}$), and the other does not as shown in Figure 32, case 2. Then η can be written:

$$\eta = \frac{G}{2}\left\{ A\left[\cos^{-1}\left(-\frac{A}{2}\right) + \frac{\pi}{2}\right] + 2\left[\left(1 + \left(\frac{A}{2}\right)^2\right)^{1/2} + 1\right]\right\} \qquad [15]$$

for $A < 1.45$ and $\widetilde{G} \to 0$, where $\frac{\pi}{2} \leq \cos^{-1}\left(-\frac{A}{2}\right) \leq \pi$.

Since η is based on the upstream area perpendicular to the flow direction, $(1 + G^2)^{1/2}$ in Nielsen's solution does not appear in Equations 13–15.

Using Equations 13–15, efficiency is plotted as a function of A in Figure 33. For $G < 0$, we can use the same approximation discussed above by substituting $\theta = -\theta$, and $G = |G|$; the efficiency for $G < 0$ is also plotted in Figure 33. It is seen that η/G does not vary greatly with respect to G. The collection efficiency for positive G increases rapidly with the induced charge parameter A. In order to predict ESFF performance correctly, one should, therefore, take proper consideration of the induced charge effect. For the ESFF of irregular fiber structures, this effect may be included empirically as a geometric factor.

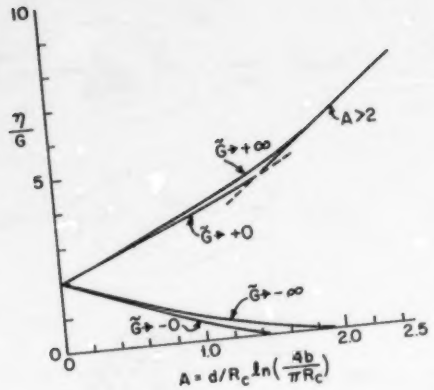

Figure 33. Collection efficiencies for charged particles on fibers with potential-induced charges.

REFERENCES

Kirsch, A., The Influence of An External Electric Field on the Deposition of Aerosols in Fibrous Filters, Aerosol Science *3*, 25 (1972).

Miller, B., G. Lamb, and P. Costanza, Influence of Fiber Characteristics on Particulate Filtration, EPA-650/2-74-043, May, 1974.

Miller, B., G. Lamb, P. Costanza, and J. Craig, Nonwoven Fabric Filters for Particulate Removal in the Respirable Dust Range, EPA-600/7-77-115, October 1977.

Miller, B., G. Lamb, P. Costanza, D. O'Meara, and J. Dunbar, Studies of Dust Cake Formation and Structure in Fabric Filtration, First Year, EPA-600/7-78-095, June 1978.

Miller, B., G. Lamb, P. Costanza, G. Harriott, J. Dunbar, and M. Mokriski, Studies of Dust Cake Formation and Structure in Fabric Filtration, Second Year, EPA-600/7-79-108, April 1979.

O'Meara, D.J., Jr., Doctoral Dissertation, Department of Chemical Engineering, Princeton University, 1979.

Nielsen, K.A., Collection of Inertialess Particles on Circular Cylinders with Electrical Forces and Gravitation, J. Coll. Interface Sci. *64*, 131 (1978).

Smythe, W.R., Static and Dynamic Electricity, McGraw-Hill, New York, 1968.

Zebel, G., Deposition of Aerosol Flowing Past a Cylindrical Fiber in a Uniform Electric Field, J. Colloid Sci. *20*, 522–543 (1965).